AN ABSTRACT OF THE THESIS OF

THOMAS VICTOR BOYLES (Name) for the MASTER OF SCIENCE (Degree)

in CIVIL ENGINEERING (Major) presented on October 17, 1969 (Date)

Title: EFFECT OF VARIABLE ROOF THICKNESS ON FALLOUT PROTECTION AND SEISMIC FORCES IN MULTISTORY STRUCTURES

Redacted for Privacy

Abstract approved: Thomas J. McClellan

Development of long-range nuclear weapons in recent years and the subsequent threat of nuclear war has led to an increased awareness of the need for civilian protection. Adequate shelter design can provide substantial protection against delayed radioactive fallout. Protection can generally be greatly increased by more massive roof construction to shield from overhead sources. Larger roof mass, however, can also greatly affect seismic loading on a structure, particularly in the case of multistory buildings. This paper reviews the nature of destructive radiation and mechanics of radiation attenuation. Fallout shelter analysis techniques are investigated as are methods of seismic structural analysis. An example multistory building is analyzed for radiation shielding potential and for seismic characteristics. Variation of these parameters is observed as a function of variable

roof mass. This study indicates that roof mass has very little effect on shielding potential in multistory structures, and that the best protection may be found in interior, or core, regions of central stories. It is further concluded that proper preliminary "slanting" in a design can provide at least minimum recommended shelter protection without varying design concepts or increasing costs.

Effect of Variable Roof Thickness on Fallout Protection and Seismic Forces in Multistory Structures

by

Thomas Victor Boyles

A THESIS

submitted to

Oregon State University

in partial fulfillment of
the requirements for the
degree of

Master of Science

June 1970

APPROVED:

Redacted for Privacy

Professor of Civil Engineering

in charge of major

Redacted for Privacy

Head of Department of Civil Engineering

Redacted for Privacy

Dean of Graduate School

Date thesis is presented October 17, 1969

Typed by Clover Redfern for Thomas Victor Boyles

ACKNOWLEDGMENTS

In June of 1967 the author was awarded a Fellowship from the Office of Civil Defense for the ensuing academic year. Without the research funds provided by this grant much of the in-depth computer analysis would have been impossible. The author wishes to thank O. C. D. for this opportunity and aid.

The author extends much thanks to his major professor, Thomas J. McClellan, who provided guidance and many suggestions during the writing of this paper. Thanks also to Joseph Grant who provided a computer program for seismic analysis of an example structure. And last, but by no means least, the author wishes to thank his wife, Adele, for her encouragement through the trials of research and writing of this paper.

TABLE OF CONTENTS

LIST OF FIGURES

LIST OF TABLES

NOMENCLATURE

A - Area of a structure or structural member

B_c - Barrier reduction factor for ceilings

B_e - Barrier reduction factor for exterior walls

B_f - Barrier reduction factor for floors

B_i - Barrier reduction factor for ground contribution through interior partitions

B_i' - Barrier reduction factor for overhead contribution through interior partitions

C_g - Total ground contribution to a detector

C_o - Total overhead contribution to a detector

e - Eccentricity ratio, W/L

D - Depth of a structure resisting lateral force

E - Shape factor, a function of e, applied to scatter geometry

G_a - Directional response for skyshine radiation

G_d - Directional response for direct radiation

G_g - Total geometry reduction factor for ground contribution

G_s - Directional response for scatter radiation

h - Height or length of a structural member

H - Height of detector above the contaminated ground plane

K - Seismic coefficient depending on structural framing system

L - Length of rectangular structure

M - Moment in structure or structural member

n - Normality ratio, $2Z/L$

S_w - Scatter fraction of wall emergent radiation that has been scattered in the wall

V - Horizontal seismic shear force

W - Lesser dimension of a rectangular structure

X - Mass thickness of a barrier in pounds per square foot. Subscript denotes roof, ceiling, floor, exterior, interior, or total overhead mass thickness

Z - Distance from detector to overhead source of radiation

Z - Seismic probability factor depending on geographical location

Δ - Deflection of a structure or structural member

ω - Solid angle fraction. Subscript denotes upper, lower, or overhead

Units:

1 curie = 3.700×10^{10} disintegrations per second

1 rad = 100 ergs per gram. Unit of absorbed dose

1 roentgen = 93.0 ergs per gram in water
= 83.8 ergs per gram in air

EFFECT OF VARIABLE ROOF THICKNESS ON FALLOUT PROTECTION AND SEISMIC FORCES IN MULTISTORY STRUCTURES

INTRODUCTION

Since World War II, continued development and subsequent military stockpiling of nuclear weaponry by several of the world's nations has posed an ominous threat of nuclear disaster. In addition to the tremendous destructive power of nuclear weapons, radioactive fallout has added a new dimension to war. As a result, efforts to protect as many human lives as possible in the event of a nuclear war has led to the study and development of nuclear fallout protection.

The Department of Defense has made many recent probability studies of hypothetical large scale nuclear attacks on the United States. These studies have been primarily to evaluate the defense network, but also provide a possibility of what to expect in terms of nuclear radiation fallout. From these studies have come lists and maps of probable target areas, potential immediate destruction in terms of lives and property, and an estimate of delayed radiation fallout intensities.

The Office of Civil Defense, under the auspices of the Department of Defense, has studied preparation for nuclear war at the civilian level. These studies include radiation shielding and fallout shelter analysis and design, as well as planned programs of survival.

The Atomic Energy Commission (13), interested principally in development of atomic energy uses, including medical, civil, industrial, and military, has also studied radiation protection. The A.E.C. is concerned with prevention of accidents and with public safety against hazards arising under these programs. Reports of this commission recommend adequate fallout protection for possible accidents arising from an increasing number and size of both research and industrial nuclear reactors.

Under Secretary of the Interior Stewart L. Udall, studies have been made by both governmental and private agencies to protect essential industries. Some of these include petroleum and gas (9), minerals and solid fuels (16), electric power (15), and airports (17). These studies basically include probable targets and effects, and survival and restoration of the industries. Survival programs outline principles and procedures in preparing for protection of raw materials and records, continued production and management, communications, and most important, instruction and protection of personnel, provision of fallout shelters, and rehabilitation. In addition, airport personnel are advised on handling radioactive materials and atomic devices, and what to do in case of emergency.

Increasing use of nuclear power for peaceful means has led to a very scientific analysis of radiation shielding. This shielding is necessary because operating personnel must be protected from the

emitting source inside the reactors. Construction materials and reactor shield configurations have been studied (10). However, because this work was primarily done by scientists and mathematicians, shielding analysis has been on a very theoretical plane involving complex equations and requiring an understanding of the physics involved to design a working shield.

In the past several years the necessity of providing nuclear fallout protection for public safety has become more apparent. As a result, the need for more simple shielding design techniques has also become necessary. Largely through efforts of the Office of Civil Defense, radiation shielding design and analysis equations are now much easier to solve (14). Easily interpretable nomographs relating building construction and geometry parameters to shielding protection capabilities replace solution of intricate mathematical relationships.

In 1960, Nelson A. Rockefeller, as chairman of a special committee of the governors' conference, reported that fallout shelter protection is feasible, whether at the individual family or group levels, and offers the best single non-military defense measure for protection of the greatest number of people (19). This protection of American citizens is also essential to military defense in seeking peace through deterrence of nuclear attack. In the event of nuclear war, casualties suffered depend not only on the character of attack, but also on extent of protective measures taken by the civilian population.

Radiation from fallout is a massive threat to both target and non-target due to wind drift of contaminated particles in the air. Two possibilities of contacting radiation contamination are external irradiation and internal consumption of contaminated food or breathing of contaminated air. The goal of radiation shielding and of this paper is to promote adequate defense against the first.

Calculation of a sufficient shield thickness requires knowledge of the following factors:

(1) types and intensities of radiation emitted from a source,

(2) rate of radiation attenuation by the shielding material, including effects of geometry and production of additional secondary re-radiation from the attenuation process, and

(3) allowable intensity for acceptable dose rate and total dosage.

These factors reflect the broad categories of simplifying assumptions that have been made in reducing a rigorous mathematical shielding approach to a workable analysis and design approach.

Due to the need for fallout protection, the Office of Civil Defense, as well as other organizations, has been trying to convince designers of the practicality of providing shelters in their buildings. The shelter areas need not be separate, massively constructed areas within or beneath the building. With a little foresight, involving choice of location and construction materials, an area can easily

become adequately protective against radiation fallout. With this "slanting" technique in mind, i.e., planning ahead to provide resistance to radiation penetration within the structure, there need be little if any change in design esthetics. Also, this protection can be provided at no additional cost with proper choice of construction materials and building geometry.

In some cases, however, increased mass of the building may necessarily be the only solution to increasing fallout protection since attenuation is directly proportional to mass weight between source and recipient. As a result of increasing the building weight, seismic forces on the structure and subsequent stresses in members may be increased. In order to provide for these greater loads, structural members may require additional size to provide adequate strength and stiffness. Although it is economically impractical to protect all structures against failure due to nuclear blast, any strengthening to provide for seismic loading will have the consequent effect of providing some additional protection against blast, if given enough distance between target area and structure.

Objectives of Study

If additional mass is required in a given building to provide adequate fallout protection, how much is necessary? What are the effects of this added mass on shielding potential in various portions of the

building? What are the effects of greater building mass on induced seismic loading and resulting stresses and deflection of the structure?

Principally, the purpose of this paper is to identify and study relationships between adequate fallout protection in multistory buildings provided by increasing the roof mass and consequent increased seismic forces, stresses, and deflections due to this increase in dead load. The objectives are first studied in theory and then in a selected multistory building example.

Through this study the author hopes in some small way to project to designers the desirability of "slanting" design objectives toward providing adequate fallout shelter protection in structures. The author will try to show that this protection can be provided without unduly altering design concepts, structural system or member sizing, or building cost.

THEORY

Nuclear Radiation Fallout

Nuclear explosions are characterized by a very rapid release of large amounts of energy within a small space (6). The energy and effects of atomic explosions are described in terms of conventional weapons, i.e., tons of TNT. Thus a 20 kiloton[1] or a one-megaton yield explosion is equivalent to the explosive energy relase of 20 thousand or one million tons of TNT respectively. These devices may be either fission or fusion types, both of which can also be thermonuclear.

A nuclear explosion involves a large increase in temperature and pressure, as well as light, sound, and radiation. An approximate constituent distribution if 50% blast and shock, 35% thermal radiation, 5% initial nuclear radiation, and 10% residual radiation (14). Both distribution and total yield depend on the type of explosion; i.e., high or low altitude, surface, or subsurface. The shock or blast wave is accompanied by a strong wind involving both over-pressure and suction if the explosion is in the air, but is characterized by an impact or impulse if the explosion is subsurface. The large temperature increase due to thermal radiation can cause fires and flesh burns at

[1] Yield of early fission atomic bombs dropped on Hiroshima and Nagasaki near the end of World War II.

large distances. A fireball touching the earth's surface causes vaporization and pulverization of large amounts of debris. This is sucked upward by temperature currents and the explosive force, carried by wind currents, and later falls back to earth in the form of radioactive fallout. All effects of the explosion decrease with distance and time from the explosion.

Nuclear radiation involves both initial and residual or delayed radiation. Residual radiation is defined as destructive nuclear radiation rays emitted after one minute from the instant of explosion (19). Residual radiation includes continuation (at a reduced rate) of initial radiation and delayed radiation in the form of fallout. Fallout particle size varies from dust to invisible depending on time and distance from ground zero. Early fallout, the most coarse of which is something like fine beach sand, occurs within 24 hours.

Radiation intensity to be expected is very difficult to estimate because the level depends on the number, power, and type of nuclear weapons, location of bursts, height above ground, nature of radioactive debris, wind, and weather. These factors are complicated by overlapping of fallout patterns from separate detonations. Estimated intensities are not likely to exceed 10, 000 roetgens[2] in two weeks,

---

[2] Unit measuring the ionization potential of x- and gamma radiation. A roentgen is defined as the quantity of x- or gamma radiation causing the formation of 2.08×10^9 ion pairs per cubic centimeter of dry air at standard temperature and pressure.

but may be temporarily greater in some scattered areas due to overlapping patterns and weather conditions (12).

Attenuation of Radiation

Radioactive material or contaminated matter decays exponentially with time, emitting penetrating electromagnetic radiation. This radiation, both invisible and odorless, is composed principally of free neutrons, alpha particles, beta particles, and gamma radiation. Free neutrons are direct components of any nuclei and may be released by either a fission or fusion process. These particles have a large mass and neutral charge. Neutrons cause no direct ionization, only new atomic products. Hence, the effects of free neutrons are limited to initial radiation and are not a primary consideration of fallout shelter design.

Alpha radiation is atomically equivalent to the nucleus of a helium atom and hence positively charged, large, heavy, and relatively slow. Alpha particles are easily absorbed in about two inches of air and it is doubtful that they could penetrate unbroken skin (14).

Beta particles are very small, negatively charged, and have low mass, but travel at very high velocity and hence are identical to a stream of electrons. More easily attenuated than electrons, however, beta particles can penetrate only 10 to 12 feet in air and can produce some radiation burns in contact with exposed skin.

Gamma radiation may be released by either a fission or fusion process, or as a product of radioactive decay. Having no electrical charge nor mass, gamma radiation is like a continuous stream of photons,[3] or pure energy, traveling at the speed of light. In this way, gamma radiation is very similar to x-rays but different in origin. Gamma rays are extremely penetrating, requiring considerable attenuating mass, and hence are very dangerous biologically.

As a result of relative penetration capabilities of radiation, fallout shielding protection is primarily concerned with the attenuation of gamma rays arising from the decay of radioactive fallout particles.

The process of attenuation of gamma rays is fairly well understood. There are three general processes involved: 1) ionic pair production, 2) the photoelectric effect, and 3) Compton scattering. The first two processes depend on atomic number of the attenuating material, that is, density of the actual atoms composing the absorbing medium. The last process involves orbital electron interactions, so depends on mass per unit area (i. e., area-density) of attenuating barrier since equal masses of most common construction materials contain approximately the same number of electrons (10).

---

[3] A photon is defined as a quantum of pure radiant energy moving at the velocity of light.

Principally then, what is required is an adequate mass of shielding material between a radioactive source (in this case fallout) and personnel. For a given level of intensity, the greater the mass of material, which includes both density and thickness, the greater the protection. Natural earth is the least expensive and most readily available of dense materials suitable for construction use. Hence building below ground level or else locating earth embankments against buildings are recommended as providing the cheapest natural protection. The use of earth, however, is not always acceptable in a given design.

Concrete is the most widely used shielding material for both reactor and fallout protection. This is due to the relative cheapness but satisfactory absorbing capabilities and good structural properties of concrete. Nuclei of the concrete matrix have a fairly high atomic number so are efficient in absorbing gamma rays and slowing down fast neutrons by scattering. Aggregates, of course, can also be selected to have high densities. In addition, the retained water of hydration absorbs thermal energy emitted as radiation releases energy on absorption.

Gamma radiation shielding properties of concrete vary with both density and thickness of the concrete. Figure 1 compares the relative absorbing potentials of several possible shielding materials (10). The "ten-folding length" is defined as thickness of material to

reduce by a factor of ten the radiation photon energy in MeV.

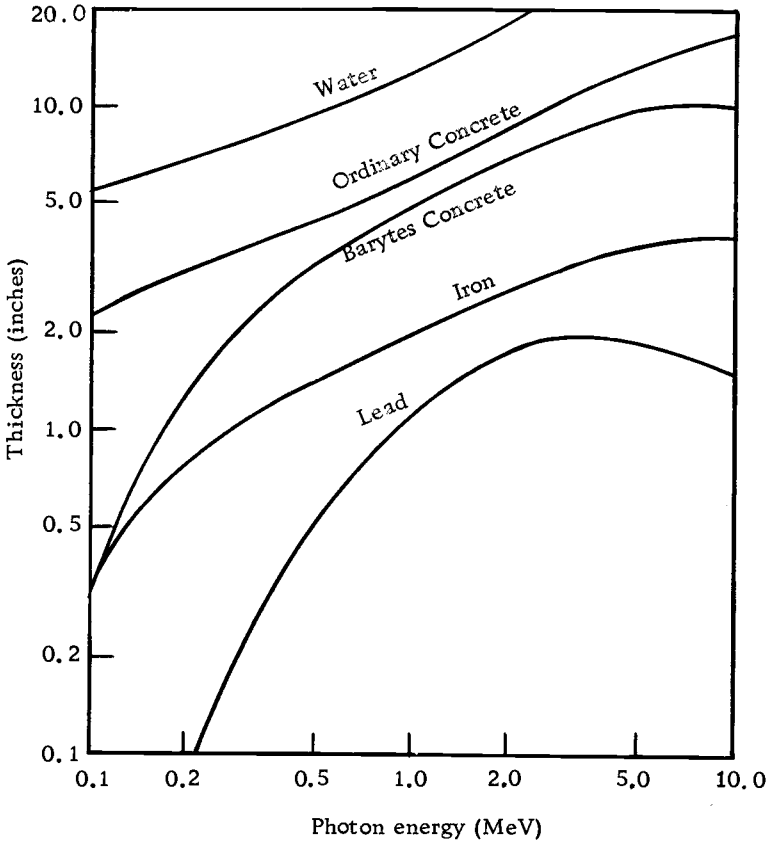

Figure 1. Ten-folding lengths for common shielding materials.

Ordinary concrete is not nearly as efficient as some other possible materials for a given thickness. Even other types of concrete, for instance Barytes, are more dense than ordinary concrete and have a better attenuation potential. Price, Horton and Spinney (10) have found that the more dense concretes are good for reactor shielding, but the extra cost is generally unjustified for most fallout protection applications. Figure 2 demonstrates how rapidly cost

increases with density of concrete due to any of several various additives (10). Relative costs including both materials and construction usually make ordinary Portland concrete the best selection over other materials for building purposes.

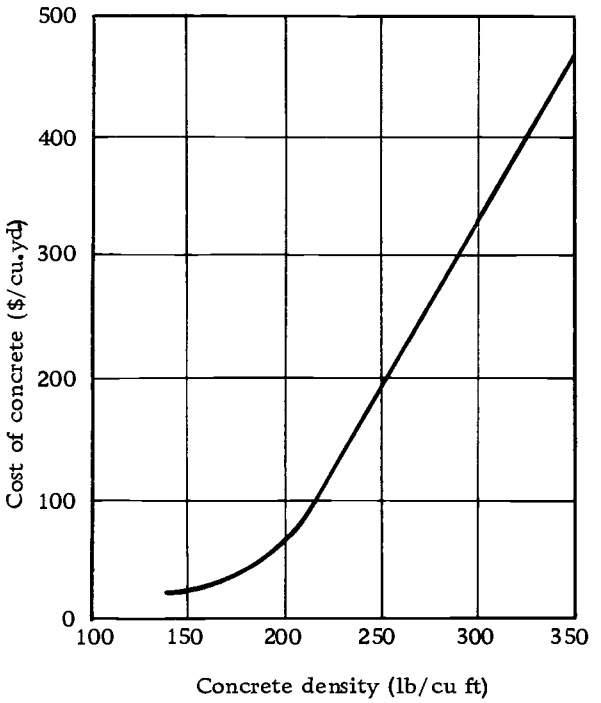

Figure 2. Approximate cost of concrete as a function of density.

Figure 3 presents a curve of experimental data showing the effect of shield thickness of ordinary Portland concrete on attenuation of gamma radiation (10). The absorption potential is nearly directly proportional to thickness but slightly nonlinear because the shield is not 100% efficient due to secondary or re-radiation of absorbed energy. Thus the greater the radiation intensity anticipated, the greater must be the shield thickness for any particular material.

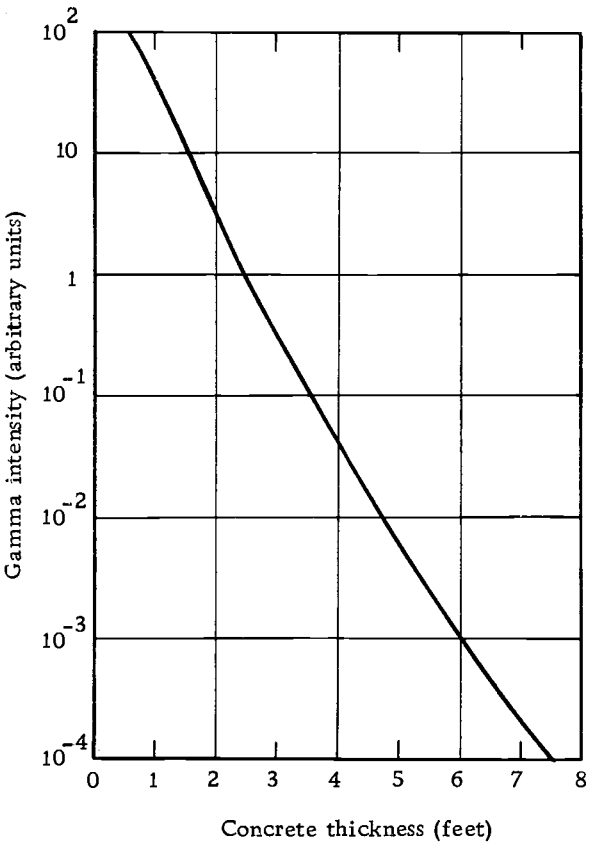

Figure 3. Effect of concrete thickness on gamma radiation attenuation.

Fallout Protection

Biological hazards of nuclear radiation have been investigated since the first case of damage in July, 1896. This was just a few months before discovery of radioactivity by Roentgen and two years before radium was separated into a pure state by the Curies. Research found that damage is not only to skin but also affects organs and bones. The roentgen was accepted in 1928 as a unit of radiation dosage.

Radiation presents two basic courses of contamination danger: 1) external irradiation, and 2) internal consumption due to ingestion (e. g. contaminated food) or breathing of contaminated air. These can only be combatted by sufficient shielding, adequate precautions, and individual care.

Fallout shelter design is based on an acceptable radiation intensity, that is, a total radiation dose permissible for human survival. An estimate of total dosage must include the combined effects of cosmic rays, natural radiation, and radiation from fallout.

Two common units of dosage measurement are the roentgen for measuring x- and gamma rays and the rad[4] for measuring alpha, beta, and neutron partical radiation. The roentgen is used to relate the radiation hazard from fallout to its biological effect on humans. Since fallout shelters consider only gamma radiation, the roentgen is a very common term in fallout shelter analysis and design. Actual physical effect on humans is measured by a unit of dosage called the rem (roentgen-equivalent-man) and is defined as the product of dose in roentgens or rads and r. b. e.[5] (relative biological effect). Normal background radiation is about 0. 0003 rem/day and everyone absorbs about 10 roentgens during his lifetime (18).

---

[4]Unit of absorbed dose, 100 ergs/gm = 1 rad.

[5]Relative biological efficiency rating of various radiations depending on ionization effect on the body.

Total dose, or accumulated dose (roentgens), is the dose rate (roentgens/hour) integrated over the time period considered. Dose rate is defined as the rate of gamma radiation received by a detector three feet above the ground or floor plane.

It is generally accepted that a total accumulated radiation dosage of about 100 roentgens over a two week or longer period will have little or no effect on a human, nor restrict his working efficiency. In some cases particular individuals may be able to continue working if the total dosage does not exceed 200 roentgens over a few days period although some nausea and vomiting will occur (10). Short term doses of 200 to 600 roentgens will cause some death, while doses greater than 1, 000 roentgens are nearly certain to be lethal. The U. S. Navy (18) recommends a permissible level of 0. 050 rem/day and 0. 3 rem/week. More than this, or less time, will probably cause radiation sickness. Time is an important factor in measuring the effects of a radiation dose since the body will repair some of the damage given enough time. The Navy also suggests a lethal radiation exposure as 400 to 600 rems in one day.

The intensity of radiation from fallout diminishes at a rapid exponential rate with time. For example, seven hours after the time of explosion, i. e., radiation release, the radiation intensity level may be only 10% of the intensity level at one hour after initial release. If time and distance are not enough to protect the particular area, the

radiation may be blocked by shielding.

As previously noted, the design of an adequate radiation shield requires the knowledge of type and intensities of radiation emitted from a source, rate of radiation attenuation by the shielding material, including effects of geometry, and an acceptable intensity level not to exceed a maximum permissable dose rate or total dosage. Determination of the relative degree of shielding protection afforded to occupants is called fallout shelter analysis. Because alpha and beta rays are so easily absorbed, the attenuation of gamma radiation constitutes the entire shielding consideration as far as fallout is concerned. Gamma radiation is extremely penetrating and very destructive biologically.

Gamma radiation incident upon a barrier can do one of three things, as shown in Figure 4, depending on interaction with the barrier material. If the photon encounters no interaction, there will be no reduction in energy and it will pass directly through the barrier. This is called direct radiation. A partial loss of energy involving incomplete photon absorption by an orbital electron will cause the photon to bounce off in a different direction at a lower energy level (Compton effect) and hence at a lower, less destructive velocity. This emerging photon is called scattered radiation. A complete exchange of energy upon interaction (photoelectric effect) is called absorbed radiation and hence there is no emergence of the photon from

the barrier.

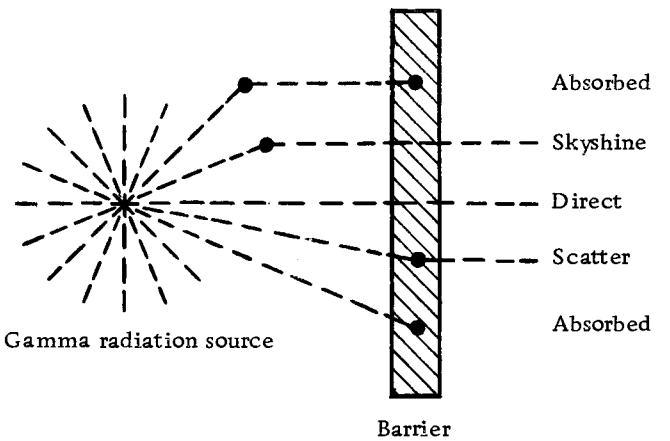

Figure 4. Barrier effects on radiation (8).

Figure 4 also shows skyshine, or albedo, radiation as a possible source in addition to the actual gamma radiation source. Skyshine is caused by the Compton effect in air. Skyshine radiation incident upon a barrier may also become direct, scattered, or absorbed radiation just as the basic gamma radiation source. About 90% of the total detector response is due to radiation from ground or overhead sources, mostly direct radiation, and about 10% from skyshine.

Whether a photon will pass directly through, be absorbed, or be scattered by the barrier depends on the energy level of the photon and number of electrons in the path to cause possible interaction. The number of electrons in the barrier is affected by both density of attenuating material and thickness of barrier. However, the ratio of atomic number to atomic mass is nearly constant for most common

construction materials (12). So mass thickness, as denoted by the parameter "X" and defined as the product of material density and barrier thickness, becomes the measure of barrier effectiveness. Mass thickness is simply the weight per unit area of barrier, generally in pounds per square foot.

Prince, Horton and Spinney (10) present very theoretical and complex, but complete, equations for shielding analysis based on a highly scientific understanding of physics. The Office of Civil Defense (14) has sought to simplify these equations by retaining essential contributing factors, and yet remaining relatively complete and safe.

In order to evaluate the effectiveness of a barrier, it is necessary to have a standard reference location for the radiation detector for a comparison. This standard has been defined as an unprotected detector located three feet above a smooth plane of infinite extent in all directions upon which fallout particles are uniformly distributed, and which measures the amount of radiation received from all directions. Radiation received at the standard, for use in the O. C. D. analysis technique, has been normalized to unity. Thus radiation received at locations protected by any shielding will be some lesser amount than received by the standard detector. This ratio is related as a decimal fraction called the reduction factor (RF).

Protection factor (PF) is defined as the reciprocal of the

reduction factor. The O. C. D. techniques for evaluating RF and PF will be followed throughout this paper.

The relative degree of protection against fallout provided by a structure as compared to the unprotected standard detector is the protection factor. Note that neither the reduction factor nor the protection factor makes any assumption of radiation intensity from the uniformly contaminated field.[6] Intensity to be expected cannot be determined exactly, only estimated. As an example, assume a protection factor of 100, available at a particular detector location, and an unprotected standard detector total dose of 15, 000 roentgens over a period of time as the source strength. Thus the protected detector would receive only 150 roentgens over this same time period. This protected detector dose is evaluated as the product of RF and the field intensity. The protection factor presents a method for comparing relative protection capabilities of different construction techniques and materials of buildings under design, or between different buildings, or locations within buildings already existing.

Calculation of the reduction factor can only be made for one specific location at a time. Radiation received by the detector must consider separately the contributions through walls and partitions,

---

[6]The uniformly contaminated field includes the ground surrounding the structure and the roof, but not floor surfaces within the structure nor walls of the structure.

aperatures,[7] and the roof. Each contribution has been reduced by the use of nomographs (14) to the product of a barrier effect (e. g. mass thickness) and a geometry effect (e. g. height, width, location). Each contribution is evaluated through the use of structure shielding parameters as will be shown.

Radiation received by a detector is categorized depending upon its source of origin. Ground contribution, C_g, originates from a contaminated plane or planes below the level of the detector. Overhead contribution, C_o, originates from a contaminated roof plane or other exterior planes above the level of the detector. For ease of evaluation, each contribution is further divided into direct, scattered, or skyshine depending on the individual character of radiation emergent for the particular barrier in question.

Ground contribution is evaluated by considering the path a photon must take in arriving at the detector location as shown in Figure 5. Direct radiation is considered only below the detector plane since it must travel in a straight line from source to detector through all intervening barriers. Scattered radiation may reach the detector from either below or above the detector plane due to interaction and subsequent change of path of the photon. Skyshine, caused by interaction of photons with air molecules, is considered only above the

[7] Windows or openings in walls or roof; considered to have zero mass thickness and hence provide no shielding effect.

detector plane.

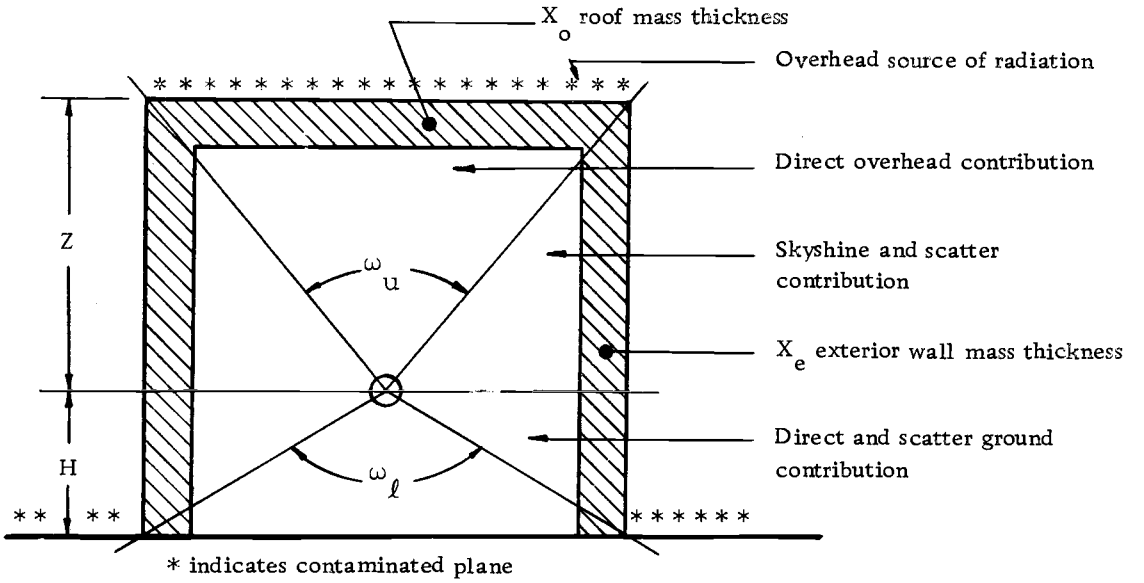

Figure 5. Zones of contribution.

Only radiation reaching the detector is considered, so much of the total radiation emerging through the barriers is neglected. Two other secondary sources are also neglected for ease of calculations. These are re-radiation from absorbed photons within the barrier and back-scatter from other surfaces within the structure. These secondary effects are usually very minor in comparison to contributions from other sources.

Overhead contribution, C_o, from sources on planes above the detector also consists of direct, scatter, and skyshine, as well as secondary sources. O. C. D. nomographs for evaluation of overhead contribution consider the first three as a single contribution and

neglect the latter.

As shown in Figure 5, contributions are evaluated by considering the portion of the structure through which the radiation must emerge to reach the detector. Thus the effect of structure geometry is important. The geometry of a particular zone of contribution is considered as a pyramidal volume defined by a base area and a cone height. This volume, also described by a solid angle fraction, ω, at the apex of the pyramid, is dependent on structure dimensions. This single parameter relates proportionately the physical dimensions to detector response. These volumes are shown in two-dimensional form in Figure 5.

This solid angle fraction is described as the apex angle of a pyramidal volume. This is actually defined as the solid angle of a cone multiplied by $1/2\pi$. Thus for a segment of a sphere,

$$\omega = \frac{A}{2\pi r^2} .$$

This definition can be extended for a rectangular volume and simplified to

$$\omega = \frac{2}{\pi} \tan^{-1} \frac{e}{n\sqrt{n^2+e^2+1}}$$

by defining the eccentricity ratio

$$e = W/L$$

and the normality ratio

$$n = 2Z/L$$

for the upper solid angle fraction, ω_u, and

$$n = 2H/L$$

for the lower solid angle fraction, ω_ℓ. The detector height, H, will commonly be three feet except for certain cases, e. g. multistory structures. Hence the solid angle fraction is dependent upon the building dimensions and detector height, and is written in functional notation[8] as $\omega(e, n)$.

Figure 5 shows the zones through which contribution must pass in reaching the detector. Thus, overhead contribution is limited to the volume described by the upper solid angle fraction, ω_u, and ground contribution enters through the barrier in the volume between ω_u and the lower solid angle fraction, ω_ℓ. This is further subdivided by considering direct, scatter, and skyshine separately. Ground direct must pass through the volume between ω_ℓ and the detector plane, while skyshine is limited by definition to the volume above the detector plane and below ω_u. Scatter radiation

[8] Functional notation is a method whereby dependent parameters involved in each term of an equation are indicated in parentheses. This technique will be utilized in most fallout shelter analysis and design equations throughout this paper.

contributes through the entire volume between ω_u and ω_ℓ.

As can be seen from the contribution zones described, total detector response will depend on structure dimensions and height of detector as defined the solid angle fractions. As ω_u increases (increase in W or L, decrease in Z), overhead contribution and lower wall contributions increase, while upper wall response decreases. As ω_ℓ increases (increase in W or L, decrease in H), upper wall response increases, while C_o and lower wall contributions decrease. Therefore the reduction factor and resulting reciprocal protection factor will vary according to detector location within a particular room. However, the detector height is usually assumed as three feet above the floor, the approximate half-height of a human.

Other important considerations include 1) variations in mass thickness, story height and building area; 2) effect of interior partitions; 3) effect of aperatures; 4) detector location; and 5) mutual shielding. The effectiveness of a barrier is directly proportional to its mass thickness. An increase in story height will decrease overhead contribution while an increase in building area will have just the opposite effect. Interior partitions place more mass thickness between the detector and contaminated field so have the effect of decreasing both ground and overhead contribution and thus increasing protection. Aperatures increase contribution and decrease protection

since they have zero mass thickness and hence no shielding ability. Mutual shielding of one building for another will decrease ground radiation (and possibly some skyshine) but has no effect on overhead contribution.

The location of a detector has a very great effect on shielding potential, particularly the height either above or below the contaminated ground plane. Ground contribution decreases as the detector moves below the contaminated plane since there is less wall height subject to exposure. A structure with the roof level at or below grade will receive no ground radiation, only overhead. As the structure becomes subsurface, the earth provides additional overhead mass thickness, thus further increasing protection.

Protection from ground direct radiation also increases in upper story locations. The slant distance between source and detector increases the number of possible interaction atoms of both air and barrier materials, effectively increasing shield thickness. Overhead contribution, however, is not merely a function of detector height above a contaminated ground plane, but rather distance of detector below a contaminated roof plane. This would suggest the possibility of greater protection somewhere toward central stories of a multistory structure.

Calculation of the ground contribution, C_g, requires first the evaluation of upper and lower solid angle fractions, ω_u and ω_ℓ, to define the volume zones through which incident radiation must pass

in reaching the detector. These are to account for the differing emergent radiation through the walls above and below the detector plane and through the roof. So a particular detector height above the contaminated plane must be selected. Detector height may vary for each set of calculations, however, as a comparison of protection between the detector locations. This comparison is particularly important in the case of multistory structures.

Mass thicknesses must be selected for each wall, interior partitions, and roof (also floors and ceilings in multistory structures) according to the weight per unit area of each. Every significant change in mass thickness or geometry should be identified and located by the appropriate solid angle fraction.

Spencer has developed a relationship between directional response and solid angle fraction for the ground contribution components (14). Ground direct (G_d) for an H of three feet, wall scatter (G_s) and skyshine (G_a) are plotted versus solid angle fraction (14, Fig. 5-7 or Chart 2). Ground direct contribution has been shown to vary with detector height above the contaminated ground plane. Thus for the case of multistory structures the correct graph must be used in evaluating $G_d(H, \omega)$ (14, Fig. 5-22 or Chart 3) depending on detector location. Both G_s and G_a are functions of ω only. The skyshine values include ceiling albedo (ceiling shine) but neither G_s nor G_d include an allowance for secondary

scattering of radiation.

Total contribution through a shield is a combination of barrier and geometry effects. The shape factor $E(e)$, a geometry effect, is a function of the eccentricity ratio $e = W/L$ and is defined by the equation

$$E(e) = \frac{1+e}{\sqrt{1+e^2}}.$$

This is a correction factor applied to G_s values to account for building shape. The shape factor is easily evaluated by a nomograph of $E(e)$ versus e (14, Fig. 5-9 or Chart 4). A barrier factor is necessary to account for mass thickness of exterior walls. This weighting factor, indicating total radiation scattered in the exterior walls but still emergent to the detector, is called the scatter fraction, $S_w(X_e)$. The scatter fraction is evaluated by a nomograph of $S_w(X_e)$ versus exterior wall mass thickness, X_e (14, Fig. 5-10 or Chart 5). Total wall scattered contribution is multiplied by $S_w(X_e)$ and the sum of direct and skyshine contributions is multiplied by $[1-S_w(X_e)]$.

The total geometry factor for ground contribution, G_g, is obtained by summation of the three contributions from ground radiation as corrected appropriately by the shape factor and scatter fraction. The ground geometry factor is given by the expression

$$G_g = [G_s(\omega_u)+G_s(\omega_\ell)]E(e)S_w(X_e) + [G_d(H,\omega_\ell)+G_a(\omega_u)][1-S_w(X_e)] \quad (1.1)$$

in functional notation.

Actual total ground contribution to the detector, C_g, is the product of the ground contribution geometry factor, G_g, and the barrier factor(s), B. These barrier factors are defined by the relative amount of radiation that penetrates a barrier relative to the total amount incident upon it. These factors are the exterior wall barrier factor, $B_e(X_e, H)$, and the interior wall barrier factor, $B_i(X_i)$. The latter is further separated into $B_i(X_i)$ for use with C_g and $B_i'(X_i)$ for use with C_o, the overhead contribution. Spencer has given these factors in the form of nomographs (14, Fig. 5-12 and 5-15 or Charts 6 and 7). Thus the total ground contribution, C_g, is given by

$$C_g = G_g B_e(H, X_e)B_i(X_i) \quad (1.2)$$

where G_g is the ground geometry factor from Equation (1.1).

The overhead contribution to detector response, C_o, is less involved in calculation than ground contribution. The radiation source is a uniformly contaminated plane on the roof or adjacent structures above the detector plane. Volume contributing to the detector is

defined by the overhead solid angle fraction, ω_u. Shielding is provided by roof mass thickness, X_o or X_r, and the sum of all other overhead shielding layers such as floors (X_f). The total overhead contribution, $C_o(\omega_u, X_o)$, is evaluated graphically (14, Fig. 5-3 or Chart 9) which includes skyshine through the roof. Interior partitions decrease radiation contribution to a detector by placing greater attenuating mass between source and detector. When interior partitions are involved, two overhead volumes must be geometrically defined: the core area, ω_o, and the peripheral area, ω_o'. The latter includes interior barrier effects. The actual radiation reaching the detector from overhead sources is given by the expression

$$C_o = C_o(\omega_o, X_o) + [C_o(\omega_o', X_o) - C_o(\omega_o, X_o)]B_i'(X_i). \qquad (1.3)$$

This equation shows how the peripheral area actually includes contribution through the core area which must be subtracted before applying the interior barrier factor.

When more than one floor is involved, as in the case of multistory structures, calculation of both overhead and ground contributions are complicated by variable detector location and a summation of barrier effects including both geometry and mass thickness. First of all, a detector location must be selected at some height above the contaminated ground plane, usually assumed as three feet above the

floor of a particular story. Since the protection factor may be analyzed for only one detector location at a time, the particular story in question is referred to as the detector story. Mass densities must be selected for each barrier. Contributing volumes must be identified and defined by solid angle fractions from the detector plane. Usually only one floor level above the detector story and one below are considered significant in contribution since mass thicknesses of floors and interior barriers are additive for each respective parameter. Also, slant distance from the source reduces contributing radiation still further. In no case is it necessary to consider more than two stories above and two stories below the detector.

Figure 6 indicates how the use of solid angle fractions has been expanded to define contributing volumes in a multistory structure. Note that C_o is necessarily greatly reduced with distance of detector from the roof source since each floor adds its own mass thickness, X_f, to the roof mass thickness, X_r, for a total overhead X_o. But the ground contribution is increased as the detector gets closer to the ground source since ground direct, a primary contributor, is a function of detector height, as indicated by $G_d(H, \omega_\ell)$.

Total ground contribution is the summation of C_g of the detector story and the stories as may be considered above and below the detector. Each story may be considered separately as the detector story with its own appropriate solid angle fractions and barrier

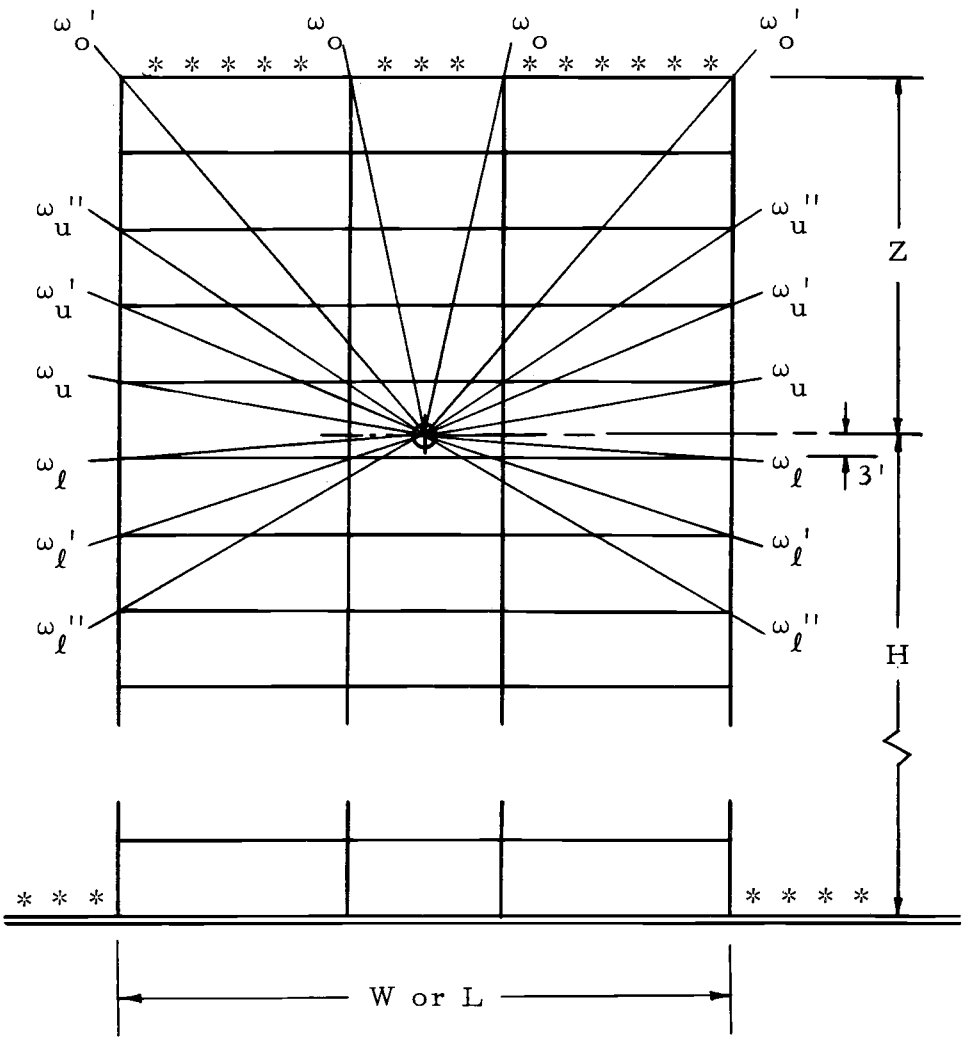

Figure 6. Typical multistory structure.

factors for best location comparison purposes.

The reduction factor is the sum of the overhead contribution and ground contribution. For multistory structures, the reduction factor must include the C_g from each story considered. The protection factor is calculated as the reciprocal of the reduction factor. Hence the protection factor, PF, is only for the particular detector location considered.

The Department of Defense has studied in detail possible radiation intensity levels. Based on recommended maximum dose rates and total doses, O. C. D. policy accepts a minimum protection factor of 40 for fallout shelters for the general public (14). O. C. D. recommends shelters for critical operations to have a minimum PF of 100.

The protection factor has been shown to depend essentially on detector location, geometry of the structure, the construction materials and techniques used, and mass thicknesses of the barriers. One or more of these factors may be varied to alter the PF as desired. Overhead contribution is very significant to total detector response in upper story locations of a multistory structure. This contribution can be reduced by moving the detector farther from the roof source (and hence increasing the ground contribution) or by increasing the mass thickness between the source and detector. This paper studies the latter method by varying the roof mass thickness of a

given structure and its effect on the PF at each floor level.

Seismic Loading on Structures

Multistory structures are subjected to both vertical and lateral loads. Vertical loads are generally static in nature and include dead loads and live loads. Lateral loads are usually dynamic and include the action of wind, earthquakes, and blast. Dynamic loads differ from static loads in that they are variable with time while the latter are constant at least over some finite length of time.

Dead loads are those generally remaining on a structure throughout its lifetime. This includes weight of the structure and any permanently attached equipment. Live loads are those of a temporary nature such as personnel, snow, merchandise, etc. These are usually static and generally assumed to be uniform over a roof or floor area. However, live loads may be dynamic and concentrated as in the case of cranes and automobiles. The Uniform Building Code, or U. B. C. (8), specifies minimum live loading, as well as other minimum loadings, to be considered for various types of structures. Local building codes often take precedence over the U. B. C. in specifying wind and snow loading.

Lateral loads, consisting of wind, seismic, and blast forces, are very statistical in nature and any loading assumed is empirical. Many studies have been made to determine loading characteristics and

effects on various types of structures. Wind forces are actually composed of an external pressure on the windward side and an external suction on the leeward side. The intensity of each constituent is directly proportional to the square of the velocity of the wind. These components have been combined into a total horizontal wind force given by an empirical equation such as $P = 0.0033V^2$ psf which corresponds to a pressure of 20 psf at 77.8 mph velocity. On most buildings, the time rate of build-up of peak wind velocity is large with respect to the natural frequency[9] of the structure. For this reason, any possible periodic "aerodynamic" forces are assumed negligible and wind forces are applied as static loads (11).

Earthquakes occur with varying frequencies and intensities throughout the world. Accelograms of several large earthquakes have been recorded. These show that ground motion is very complex and irregular in magnitude, direction, period, and acceleration. The coastal areas of California are generally assumed to be the most critical seismic areas in the United States. However, three of the largest, most destructive earthquakes have occurred from coast to coast. The San Francisco earthquake of April 18, 1906 was characterized by horizontal displacement along a vertical fault plane. New

[9]Natural frequency is defined as the number of cycles per unit time of free vibration, that is, vibration after the force causing motion has been removed or has ceased to vary. The common unit is cycles per second, cps.

Madrid, Missouri was the epicenter of a Mississippi Valley earthquake in 1811 that had a large vertical displacement over an area of more than 30, 000 square miles. In 1886, Charleston, South Carolina experienced the worst earthquake in history in the eastern United States (11).

Statistical studies of many accelogram recordings reveal no possible established pattern of intensity to expect. Instead it is suggested to use either the El Centro, California accelogram, one-tenth the natural acceleration of gravity (4), or a static loading given by building codes (e. g. U. B. C.).

Blast forces involve very large and elusive loads occurring over a short time period, so obviously any assumed blast load for analysis is only approximate. Often either vertical loads, or allowable unit stresses as applied to vertical loads, are modified to account for the limited duration of blast loads (11). The designer must be particularly careful of brittle fracture caused by the sudden application of large loads.

It is uneconomical to design structures so that failure is impossible under all possible lateral loading conditions. Structures are in general lateral force resisting (particularly regarding earthquakes), not failure proof. Multistory structures with many degrees of indeterminancy provide an additional safety factor in over-stressed loading conditions since redundant and less-stressed members will assume

more load as stresses are distributed throughout the structure. Also joints and members will yield plastically, where possible, helping to prevent collapse. However, stability of the structure must also be checked, particularly as overstress and deformation begin to occur.

Dynamic lateral forces involve motions that are random and chaotic in nature. Seismic movements involve all six degrees of foundation freedom, three translational and three rotational. Dynamic disturbances are associated with displacement of the structure due to translation, rotation, velocities, and accelerations. These disturbances are assumed to occur in the foundation for earthquake analysis. Of course the magnitude of each of these necessarily varies with time.

Analysis of a structure subjected to dynamic loads consists primarily of the determination of the time variation of deflection from which stresses can be directly computed. This requires first a known or assumed load-time relationship called the load function. The natural period[10] is computed as a function of mass and stiffness of the structure. Time variation of deflection may be computed by either approximate or rigorous analysis techniques. Dynamic stresses can be computed at any point in time knowing the time-history of deflection. For example, the simple relationship of maximum column

---

[10] Natural period, the reciprocal of natural frequency, is defined as the length of time for one complete cycle of free vibration.

bending moment to relative deflection between member ends is given by

$$M = \frac{6EI\Delta}{h^2}$$

for a framed structure with rigid joints. Approximate or numerical dynamic analysis techniques are generally iterative processes and include the following: 1) constant-velocity or lumped-impulse procedures, 2) linear acceleration method, 3) Newmark β method, and 4) finite difference method. More exact rigorous analysis techniques approximate a closed form solution to give displacement as a function of time. These methods include: 1) the Stodola-Vianello procedure for natural frequencies, 2) the modified Rayleigh method for natural frequencies, 3) LaGrange's equation, and 4) modal analysis (4). The latter two techniques are greatly aided by the use of matrices.

Dynamic analysis is further complicated if the structure is unsymmetrical in plan since the resultant lateral load will probably not pass through the shear center.[11] This will cause the structure to twist, each bent according to its own torsional rigidity. These torsional moments will cause distortion of the structure in addition to

[11] The shear center or center of twist for any transverse section of a beam is the intersection of the bending axis and plane of the transverse section. This is the axis through which transverse bending loads must pass to prevent torsional twisting of the beam.

deflection. Thus the analysis becomes necessarily three dimensional instead of two dimensional and consequently much more complex.

Structural frames can be analyzed in either two or three dimensions depending upon the configuration and assumptions made (7). Beams and columns are simplified to their centroidal axes and are represented as single line structural components. This is justified since stress intensities are usually nearly symmetrical about the centroidal axis. This is true of flexural and tension-compression members but will vary with components subjected to both flexural and axial loads. But since most analysis techniques are based on the small deflection theory[12] this presents no particular limitations when considering only first order effects.

Design of indeterminate structures can become a complex iterative process depending on completeness of analysis desired and limiting simplifying assumptions. The usual design sequence is from assumed member properties, to rigidities, to moments, stresses and deflections, to member sizes, and then re-analysis. Following static design and analysis, the structure may be analyzed and checked for dynamic structural integrity.

Before electronic computers, the more exact analysis of complex framed structures was very limited and difficult. Now the

[12]The small deflection theory assumes that stresses and member dimensions are not significantly altered in the deflected configuration.

designer can study in three dimension any structural configuration, member size and shape, and joint variation. Concise matrix techniques are very good for computer analysis of complex frames.

Modern structures tend to be lighter and more structurally daring. This results in more flexible structures causing longer natural periods and hence greater seismic stresses and deflections under lateral loads. Inelastic behavior of structures, particularly of ductile moment-resisting frames, is important since it is generally impractical and uneconomical to design buildings to remain completely elastic when subjected to all possible seismic occurrences. Much energy, however, may be absorbed with possibly only a small amount of joint and/or structural yielding (3). Therefore, allowing for possible plastic deformation in extreme cases results in lighter and hence less expensive structures.

The Atomic Energy Commission (12) recommends reinforced concrete frames or steel frames for multistory structures. These frames should provide the necessary rigidity to resist forces, adequate redundancy of members, and sufficient ductility to resist brittle fracture and absorb energy plastically if necessary. The A. E. C. also suggests assuming a wind pressure of 90 psf horizontally and 70 psf vertically for blast protection against structural collapse of critical structures for a 20 kiloton yield weapon three-quarters of a mile from ground zero.

The Uniform Building Code (8) is the most widely accepted building code in the United States today. This code provides simple empirical equations for seismic analysis. Seismic forces are reduced to static lateral loads to be applied at each floor level as determined by the percentage of total dead weight occurring at that particular level. These equations are based on an empirical or semi-rational approach from statistical studies of structural behavior. Horizontal shear at a particular floor level is due to a percentage of gravity acceleration and the dead load above the given story height. These loads are only a rough approximation but enable the structure to be analyzed much more easily than other methods.

The U. B. C. provides equations for computing both shear and overturning moment on the structure. The shearing force, or total base shear, to be applied at the base of the structure is given by

$$V = ZKCW \tag{2.1}$$

where W is the total dead weight of the structure and Z, K, and C are coefficients as provided by the U. B. C. The type of structural resisting system determines K (varies from 0. 67 to 3. 00) while Z (0. 25, 0. 50, or 1. 00) depends on geographical location. The value of C is determined by

$$C = \frac{0.05}{\sqrt[3]{T}} \tag{2.2}$$

where T is the fundamental period of vibration from

$$T = \frac{0.05\, h_n}{\sqrt{D}} . \qquad (2.3)$$

The total lateral force V is distributed over the height of the structure with

$$F_t = 0.004\, V\left(\frac{h_n}{D}\right)^2 \qquad (2.4)$$

being the force at the top and

$$F_x = \frac{(V - F_t) w_x h_x}{\sum_{i=1}^{n} w_i h_i} \qquad (2.5)$$

the force at any floor level "x" above the base.

Moments in the structure at a particular story, as given by the U. B. C., are determined statically based on the distributed lateral forces as computed above the given height. The moments are given as an overturning moment about a particular reference point. The total overturning moment about the base is given by

$$M_o = J\left(F_t h_n + \sum_{i=1}^{n} F_i h_i\right) \qquad (2.6)$$

where the coefficient J is defined by

$$J = \frac{0.5}{\sqrt[3]{T^2}}$$

with T being the natural period as previously computed. The overturning moment at any level "x" is given by

$$M_x = J_x[F_t(h_n - h_x) + \sum_{i=x}^{n} F_i(h_i - h_x)] \qquad (2.7)$$

where

$$J_x = J + (1-J)(\frac{h_x}{h_n})^3 . \qquad (2.8)$$

Deflection of multistory, multiple bay frames can easily be determined by either the cantilever or portal methods of analysis if the lateral forces are known or assumed. Both methods are approximate and make simplifying assumptions of location of points of contraflexure in columns and beams and of stress distribution in the columns (7).

A more exact dynamic analysis of any structure may be accomplished through the use of modal analysis techniques. Motion of the structure may be described in terms of normal, or orthogonal, modes of vibration. Nodal points, or mass points in the lumped-parameter methods, are established at various points of the structure. Each node is restrained or allowed to move in accordance with the

structural model. A total of six degrees of freedom are possible at each node in two dimensions and nine d. o. f. in three dimensions. Thus it is not uncommon to require 200 to 500 total degrees of freedom to describe a structural system. This would of course be impossible without the use of matrices plus electronic computation and a fairly substantial computer interpretive routine.

Modal analysis techniques begin with the general equation of motion

$$[m]\{\ddot{q}\} + [c]\{\dot{q}\} + [k]\{q\} = \{F_t\} \qquad (3.1)$$

in generalized system coordinates and matrix notation, where $[m]$, $[c]$, and $[k]$ are the respective matrices of mass, damping, and stiffness. The time-dependent forcing function is described by the column matrix, $\{F_t\}$. LaGrange's Equations of dissipative and resistive energies can be used to evaluate the damping and stiffness matrices, respectively. However, in large models it is easier to evaluate the stiffness matrix using discrete structural elements and lump stiffnesses at the nodal points. A diagonal, or uncoupled, mass matrix $[m]$ causes the damping and stiffness matrices to be coupled and full and, in fact, completely symmetric.

The general equation of motion can be placed in principal coordinates by the definition

$$\{q\} = [\phi]\{p\} \qquad (3.2)$$

where $[\phi]$ is the modal matrix, or array of nodal amplitudes corresponding to each normal mode. Substitution into Equation (3.1) yields

$$[m][\phi]\{\ddot{p}\} + [c][\phi]\{\dot{p}\} + [k][\phi]\{p\} = \{F_t\} \tag{3.3}$$

or

$$\{\ddot{p}\} + \lceil(\omega_n/Q)\rfloor\{\dot{p}\} + \lceil(\omega_n^2)\rfloor\{p\} = \lceil M\rfloor^{-1}[\phi]^T\{F_t\} \tag{3.4}$$

where

$$\lceil M\rfloor = [\phi]^T[m][\phi]$$

is the generalized mass,

$$\lceil C\rfloor = [\phi]^T[c][\phi] = \lceil M\rfloor\lceil(\omega_n/Q)\rfloor$$

is the generalized damping, and

$$\lceil K\rfloor = [\phi]^T[k][\phi] = \lceil M\rfloor\lceil(\omega_n^2)\rfloor$$

is the generalized stiffness. The Quality Factor is defined by $Q = 1/2\zeta$ where the damping ratio $\zeta = c/c_r$ relates the proximity of structural damping to critical damping. The resonant circular frequency for each mode is denoted by ω_n.

For the low damping ratios encountered in structural problems, damping may be ignored in computing natural, or resonant, frequencies. Considering only the case of free vibration, i.e., $\{F_t\} = 0$, Equation (3.1) becomes

$$-\omega_n^2[m]\{\phi\} + [k]\{\phi\} = 0$$

or

$$[k]^{-1}[m]\{\phi\} = \frac{1}{\omega_n^2}\{\phi\}.$$

This can also be expressed as

$$[[D] - \lambda[I]]\{\phi\} = 0 \tag{3.5}$$

where the "Dynamic Matrix" is defined by

$$[D] = [k]^{-1}[m].$$

Equation (3.5) is now in the proper form for extraction of eigenvalues λ, where

$$\lambda = 1/\omega_n^2$$

with corresponding eigenvectors $\{\phi\}$ of orthogonal modes located in the modal matrix $[\phi]$. Natural frequencies of the structure are given by

$$\{f_n\} = \frac{1}{2\pi}\{\omega_n\}$$

in cycles per second.

Equation (3.4) can now be used to develop system transfer functions which relate response at any node to applied force at any node, much like a matrix of influence coefficients. Note that thus far nothing has been required of the forcing function. Resonant frequencies

and nodal participation are dependent only on structural properties, and in particular, mass and stiffness. If a time-variant forcing function is now assumed, it is a simple matter to compute structural response in terms of deflection, velocity, and acceleration at each and every nodal point.

Lateral deflection of a multistory structure decreases with stiffness and increases with applied lateral force. Seismic forces applied to a structure are directly related to the mass of that structure. Therefore, increasing the mass of a structure, and in particular increasing the mass in upper stories, can greatly increase deflection, stresses, and distortion due to seismic loading. These effects can only be lessened by increased stiffness of the structure due to increased member size or increased aspect ratio of either bays or structure.

Summary

This paper studies the effects on radiation fallout protection factor and increased seismic loads due to variations in roof thickness in multistory structures. Increasing the mass thickness of various building components will increase the protection factor. This increase in dead weight of the structure will, however, also result in greater lateral seismic forces on the structure.

Increasing the thickness of the roof will provide more

attenuation potential of overhead contaminated sources. This increased absorption will decrease overhead contribution, thereby increasing the protection factor of the floors for which C_o has a significant effect.

In multistory structures, the upper floors will be more influenced by the overhead contribution while lower floors will be more influenced by the ground contribution. Ground radiation produces a detector response from ground direct, scatter, and skyshine effects. The first two of these will be greatly reduced after just a few stories above the ground due to the combined effects of total mass thickness and slant distance from the source. Skyshine will decrease slowly with height but is not generally a major response source. Overhead contribution will decrease rapidly with distance below the roof since each intervening floor adds its own mass thickness to X_o, the total overhead attenuating mass thickness.

Therefore, the central stories of a multistory structure, little affected by ground radiation and greatly shielded by upper floors, are probably not significantly affected by increases in the roof thickness. The protection factor in central stories should be fairly constant regardless of the roof mass thickness.

Seismic forces are particularly sensitive to increases in dead load at some significant height above the ground. So in a multistory structure, an increase in roof thickness could result in greatly

increased seismic forces. This will also induce greater member stresses and increased horizontal deflection of the structure.

In summary, this paper studies the effects of increased roof thickness on protection factor and seismic conditions. The protection factor will increase in the upper stories with increases in roof mass, but little change is expected in central and lower stories. Increasing the roof thickness will cause greater horizontal seismic forces, greater deflection, increased member stresses, and a longer fundamental period. These effects will be quantified and compared by the use of an example multistory structure.

ANALYSIS OF BUILDING EXAMPLE

To study the effects on seismic behavior and fallout protection factor due to increases in roof thickness, a multistory building example will be analyzed. The purpose of this example is to ascertain, within the scope of this paper, the validity of the theory as presented.

Description of Building

The building example selected is a "typical" multistory office building. The basic structural system is a ductile, moment-resisting steel frame repeated in equal bays. Steel truss joists covered with thin concrete and metal forms compose the floor systems. The building exterior is completely wrapped with a curtainwall covering. All structural steel is adequately protected against fire as specified by building codes. All steel framing joints are rigid and completely moment-resisting.

The building, as shown in Figure 7, is four bays long and three bays wide, each bay being 40 feet. The structure has eight stories, each 10 feet in height. So the building is a total of 120 feet wide by 160 feet long by 80 feet high.

All loads on the building are as recommended by the Uniform Building Code (8) and the reference location is some city in the state of Oregon. A uniform live load of 100 psf is recommended on each

floor for office personnel. A horizontal wind force is distributed over the height of the building at 15 psf for the lowest 30 feet of height, 20 psf for the next 20 feet, and 25 psf for the top 30 feet. From the construction materials specified, a uniform floor load of 50 psf is assumed for each floor and ten psf for the exterior curtainwall finish. Seismic forces, both shear and overturning moments, are computed from the U. B. C. design equations.

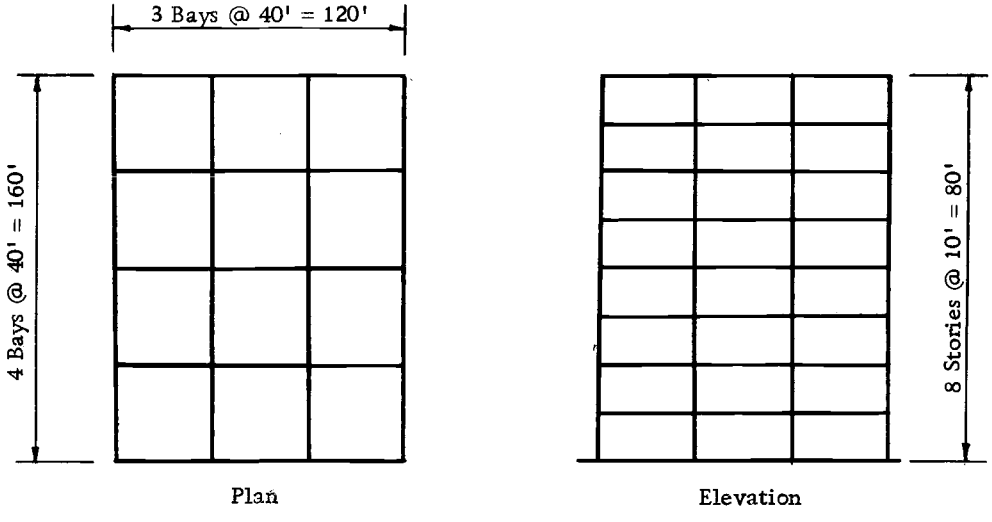

Figure 7. Plan and elevation of example building.

Protection Factor Analysis

The techniques of fallout shelter design and analysis (14) have been described previously. These methods were used to compute the protection factor of the building example for a detector location at each floor level for a variable roof thickness. This requires first of all an identification of building dimensions, geometry, and mass

thickness of each building element.

From actual physical characteristics of the example structure the solid angle fraction, ω, is computed to locate each change in geometry and mass thickness. A simple computer program was developed to calculate the eccentricity ratio, the normality ratio, and the solid angle fractions for each detector location. Input consisted of the physical dimensions of the structure as follows:

W = 120'	e = W/L
L = 160'	n = 2Z/L
H varies depending on detector story considered	
Z varies depending on detector story considered	

Results are given in Tables A-1 through A-8 in the Appendix.

The mass thickness of each shielding element was established as 40 psf for every floor except the roof and 25 psf for interior partitions including possible moveable partitions. For the curtainwall a "smeared" value of ten psf was used and the roof mass thickness was varied between 0 and 200 psf.

With the solid angle fractions determined, the scatter (G_s) and skyshine (G_a) components of ground radiation can be obtained from nomographs in the O. C. D. manual (14). Likewise the ground direct response (G_d) can be evaluated by considering detector height above the contaminated plane in addition to each solid angle fraction.

The building shape factor is determined as a function of eccentricity. Barrier factors and the scatter fraction are evaluated from appropriate nomographs by considering the mass thickness upon which each is dependent. These results are as follows:

X_o = variable	$B_e(H, X_e)$ = variable
X_f = 40 psf	$B_i(X_i)$ = 0.560
X_c = 40 psf	$B_i'(X_i)$ = 0.425
X_i = 25 psf	$B_c(X_c)$ = 0.100
X_e = 10 psf	$B_f(X_f)$ = 0.105
$E(e)$ = 1.395	$B_c'(\Sigma X_c)$ = 0.019
$S_w(X_e)$ = 0.18	$B_f'(\Sigma X_f)$ = 0.033

Probably only one floor above the detector story and one floor below need be considered. Stories outside this range are reduced greatly in contribution due to a summation of barrier mass thicknesses. Thus, the reason for notations B_c' and B_f'; to account for the double floor thickness of 80 psf for contribution from the second floors above and below the detector story. A comparison can be made to determine if additional story considerations are in fact negligible.

Calculations for ground radiation contribution to the particular detector location considered were made with the following set of equations:

1) detector story:

$$G_g = [G_s(\omega_u)+G_s(\omega_\ell)]E(e)S_w(X_e) + [G_d(H,\omega_\ell)+G_a(\omega_u)][1-S_w(X_e)] \quad (4.1)$$

$$C_g = G_g B_e(H, X_e)B_i(X_i) \quad (4.2)$$

2) first story above:

$$G_g = [G_s(\omega_u')-G_s(\omega_u)]E(e)S_w(X_e) + [G_a(\omega_u')-G_a(\omega_u)][1-S_w(X_e)] \quad (4.3)$$

$$C_g = G_g B_e(H, X_e)B_i(X_i)B_c(X_c) \quad (4.4)$$

3) second story above:

$$G_g = [G_s(\omega_u'')-G_s(\omega_u')]E(e)S_w(X_e) + [G_a(\omega_u')-G_a(\omega_u)][1-S_w(X_e)] \quad (4.5)$$

$$C_g = G_g B_e(H, X_e)B_i(X_i)B_c'(\Sigma X_c) \quad (4.6)$$

4) first story below:

$$G_g = [G_s(\omega_\ell')-G_s(\omega_\ell)]E(e)S_w(X_e) + [G_d(H,\omega_\ell')-G_d(H,\omega_\ell)][1-S_w(X_e)] \quad (4.7)$$

$$C_g = G_g B_e(H, X_e)B_i(X_i)B_f(X_f) \quad (4.8)$$

5) second story below:

$$G_g = [G_s(\omega_\ell'') - G_s(\omega_\ell')]E(e)S_w(X_e) + [G_d(H, \omega_\ell'') - G_d(H, \omega_\ell')][1 - S_w(X_e)] \quad (4.9)$$

$$C_g = G_g B_e(H, X_e) B_i(X_i) B_f'(\Sigma X_f) \quad (4.10)$$

These equations are evaluated for each floor of the example building at a detector height of three feet above the particular floor being considered. For each detector story the results are summed for a total ground contribution. This is in effect a reduction factor provided by the structure against radiation from the uniformly contaminated ground plane. Results of these calculations are shown in Tables A-1 through A-8 in the Appendix. A summary of the results is given in Table 1 for each story, showing relative contributions from stories above and below the detector story.

Detector response from a contaminated plane above the detector is called overhead contribution. Radiation from this source is attenuated by the roof and any intervening floors and partitions between the source and detector. Hence, interior partitions must be located by solid angle fractions to differentiate core from peripheral response. Due to increased slant distance and interior partition mass thickness peripheral radiation is necessarily less than core radiation.

Overhead contribution to the detector is computed with the

Table 1. Ground contribution to detector story.

Story	Detector story	First above	First below	Second above	Second below	Total C_g
8	0.013405	----	0.002634	----	0.000875	0.016915
7	0.014718	0.001112	0.003030	----	0.000961	0.019821
6	0.015370	0.001176	0.003542	0.000171	0.000981	0.021824
5	0.016984	0.001271	0.004080	0.000185	0.001243	0.023763
4	0.019491	0.001398	0.005358	0.000203	0.001332	0.027784
3	0.025363	0.001589	0.006957	0.000231	0.001402	0.035541
2	0.038743	0.001843	0.009328	0.000268	----	0.050182
1	0.099023	0.002478	----	0.0003604	----	0.101862

following equation:

$$C_o = C_o(\omega_o, \Sigma X_o) + [C_o(\omega_o', \Sigma X_o) - C_o(\omega_o, \Sigma X_o)]B_i'(X_i) \qquad (4.11)$$

Mass thickness of the roof is varied from zero (no roof at all) to 200 psf in steps of 25 psf. For a concrete of 150 pcf this corresponds to studying attenuation capabilities of the roof slab with two-inch increases in thickness up to a total of a 16-inch roof slab. Roof thicknesses of these extreme magnitudes are, of course, ridiculous, but serve merely as an academic demonstration.

Results of computations for overhead contribution are presented in Table A-9 of the Appendix. The overhead contribution for each detector story is shown in the table to be variable with roof mass thickness as was expected.

Overhead contribution as computed is added to the ground contribution for a total detector reduction factor at each detector story. This relationship is given by

$$RF = C_o + \Sigma C_g$$

where the total C_g is provided by Table 1. The protection factor is, of course, merely the reciprocal of the reduction factor. Reduction factors and protection factors are tabulated in Table A-9 of the Appendix. Results of these computations will be discussed in the

next chapter.

Structural Analysis

Objectives of a structural analysis include the determination of stresses in members, deflection of members, relative displacement of the ends of members, and stability of each component and the structure as a whole.

A multistory structure contains many members and joints, many degrees of freedom, and is usually manydegrees indeterminate. A precise analysis usually must include three dimensional considerations. A two dimensional analysis ignores torsional moments that develop due to joint rotations and a non-symmetrical plan. This latter approach greatly simplifies calculations, however, and is usually satisfactory since these stresses are generally small compared to shear and flexure (5).

In this paper, the concern is with seismic analysis of the structure and not general structural analysis. Factors in earthquake analysis include both structural and seismic characteristics. Principle properties of the building are strength, stiffness, mass, natural period, and damping effects. A seismic disturbance must consider force, amplitude, direction, and duration of the earthquake impulses. Earthquake expectations are necessarily statistical in nature and hence not nearly as accurate as estimated dead loads.

Earthquakes cause support motion, i. e., velocity and acceleration of the foundation (14). This energy is applied to the building and is absorbed in the super- or substructure in elastic or plastic flexural deflection. This deflection involves shearing action, rocking motion of the building, and possible damage to the structural system. Seismic analysis can become very complex without simplifying assumptions.

Common structural analysis assumptions are that the material is homogeneous and isotropic, that stresses are within the elastic range (i. e., Hooke's law applies), the small displacement theory, and surface effects, or contact stresses of external loads and reactions are negligible (2). Ultimate strength or inelastic stresses may be included in the cases of concrete or steel, respectively. Use of the plastic stress range becomes important in seismic analysis because of large, unpredictable loads applied over a short time interval. It is uneconomical to resist all possible lateral loads without providing for some plastic deformation to absorb energy beyond elastic capability.

Building design codes for seismic analysis are based on statistical earthquake strength and occurrence probability depending on geographical location. Codes provide approximate but relatively uncomplicated analysis procedures based on study and experience. This may be uneconomically conservative in some cases but can also serve

as a guide and rough-cut approximation when using more complete analyses. Codes such as the Uniform Building Code (8) assume a characteristic shape of the fundamental mode as a straight vertical line from top of structure to foundation (11). This is based on the assumption that total distortion of a building is the sum of shear distortion in stories of the frame and a change in length of columns due to overturning moment of the structure as a vertical cantilever. These effects combine to approach a straight line for the fundamental mode shape as assumed. It has already been pointed out, however, that structures in general, and in particular multistory structures, have as many possible modes of vibration as degrees of freedom.

Electronic computers are excellent for the solution of structural systems with multiple degrees of freedom and multiple indeterminateness. These problems involve many simultaneous equations applying the conditions of static equilibrium and compatability. Computers are much faster and, hopefully, error-free, requiring fewer simplifying assumptions.

A computer program was provided by Joseph Grant to analyze a framed structure for both vertical and horizontal loads. This program uses the matrix modal approach which is a mathematical technique for formulation of structural analysis problems. The method of matrix iteration (or method of Stodola and Vianello) is also excellent for determining vibrating frequencies of an elastic system.

Grant's program determines the lowest natural period and corresponding normal mode shape by relatively exact methods, but requires lateral forces to be applied statically. Lateral live loading conditions are, of course, not static in nature. The U. B. C., however, provides approximate static lateral loads for both earthquake and wind. Another limitation of the program was that the structure could only be analyzed in two dimensions, i. e., one frame at a time.

The example structure as analyzed is shown in Figure 7. Each side of the building is symmetrical although the plan is not. There should be little error due to torsion effects if any one frame is selected for analysis.

The particular two-dimensional frame selected for analysis is shown in Figure 8. This is an eight-story, four-bay frame, 160 feet wide by 80 feet high. Two degrees of freedom were considered at each joint, rotation and translation, or lateral displacement, for a total of 48 d. o. f. as indicated. Axial shortening of columns was neglected as being small compared to translation and rotation. Relative moments of inertia of structural members are shown in Figure 9, with a base I_o of 60 in^4. The actual moment of inertia of any particular component may be determined as the product of I_o and the relative stiffness indicated. Initial member stiffnesses were determined by a very approximate preliminary static analysis. These values were later adjusted following computer analysis to decrease

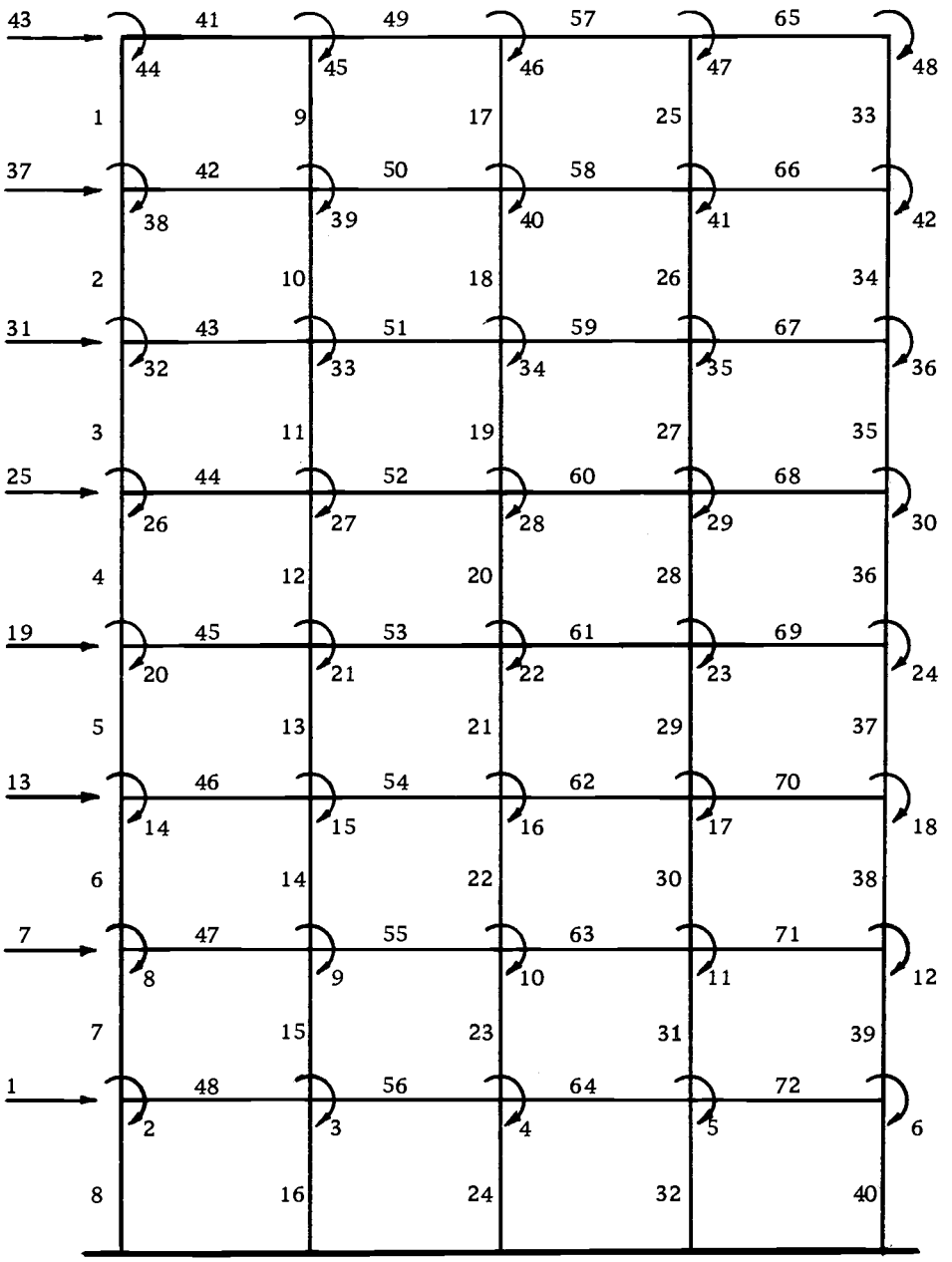

(Note: figure not to scale)

Figure 8. Two-dimensional frame showing degrees of freedom considered.

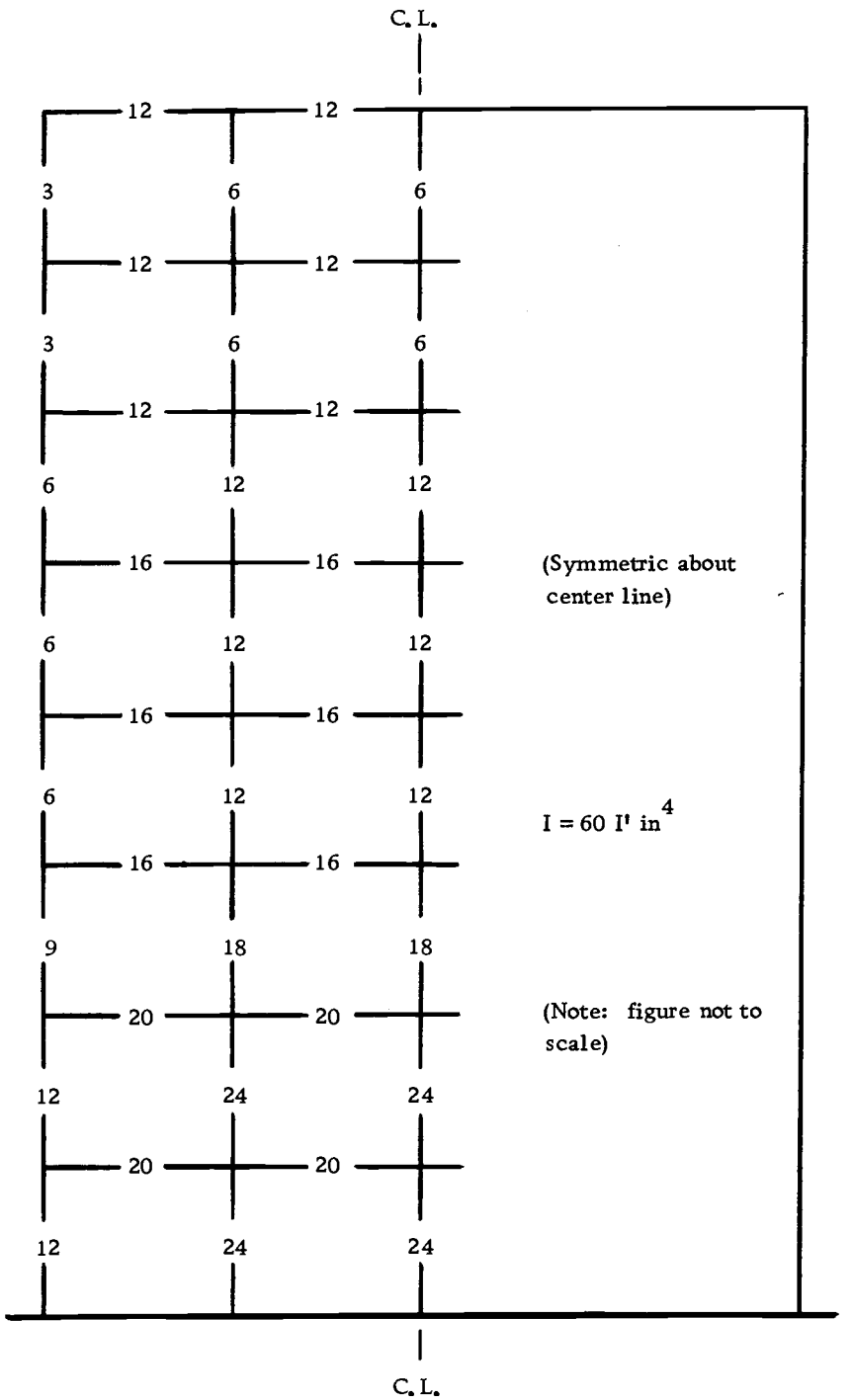

Figure 9. Relative member moments of inertia.

total deflection and either increase or decrease maximum member moments as necessary. Figure 9 indicates the final stiffness values selected for seismic analysis.

A small computer program was developed to calculate equivalent lateral seismic forces and overturning moments according to the U. B. C. equations presented previously. Results of these computations are not tabulated but are presented in Figures 12, 13, and 14. The distributed lateral seismic forces were applied at each floor level and at the roof; degrees of freedom 1, 7, 13, 19, 25, 31, 37, and 43 of Figure 9.

Structural properties, member rigidities, "static" seismic forces, and dead loads were input to the earthquake analysis computer routine. A value of 30.0×10^6 lb/in^2 was used for Young's Modulus for steel. Minor adjustments were made to relative member stiffnesses as necessary for reasonable values of total building deflection and flexural stress limitations of members. Results of the analysis are presented in Table 2 for varying roof thickness in pounds per square foot. These results are also shown in Figures 15, 16, and 17. Relative member rigidities could have been further adjusted to alter these values as required but design of the structure is not within the scope of this study.

Table 2. Seismic analysis results summary.

Roof mass thickness, X_r (psf)	Natural period (seconds)	Max. seismic deflection (inches)	Maximum moment (ft-kips)
25	0.52	1.01	537.4
50	0.57	1.02	543.6
100	0.65	1.06	562.9
150	0.73	1.12	587.9
200	0.80	1.22	616.5

DISCUSSION OF RESULTS

The multistory office building as selected for an example was analyzed for radiation fallout protection capabilities by the O. C. D. techniques. Reduction factor results were presented in Table 1 for the ground contribution alone. Table A-9 in the Appendix tabulates overhead contribution for roof thicknesses varying from 0 to 200 psf. A mass thickness of zero represents no roof at all, in effect displacing the roof plane to the eighth story floor plane. This is, of course, a very impractical situation and is presented only as an extreme example of roof thickness.

Table A-9 also presents the sums of total ground and overhead contributions as a single series of reduction factors. The reciprocal of each reduction factor provides the building protection factor for the protected detector as a function of roof mass thickness. This detector is located three feet above the floor plane of each story within the structure. These protection factors versus the corresponding roof mass thickness are presented graphically in Figure 10 for each detector story.

Figure 10 indicates how the protection factor at any given story of the building varies with roof thickness. Upper stories are more greatly changed as expected. The top floor has an increase in protection factor of 980% in a change of 25 to 200 psf of the roof, while the

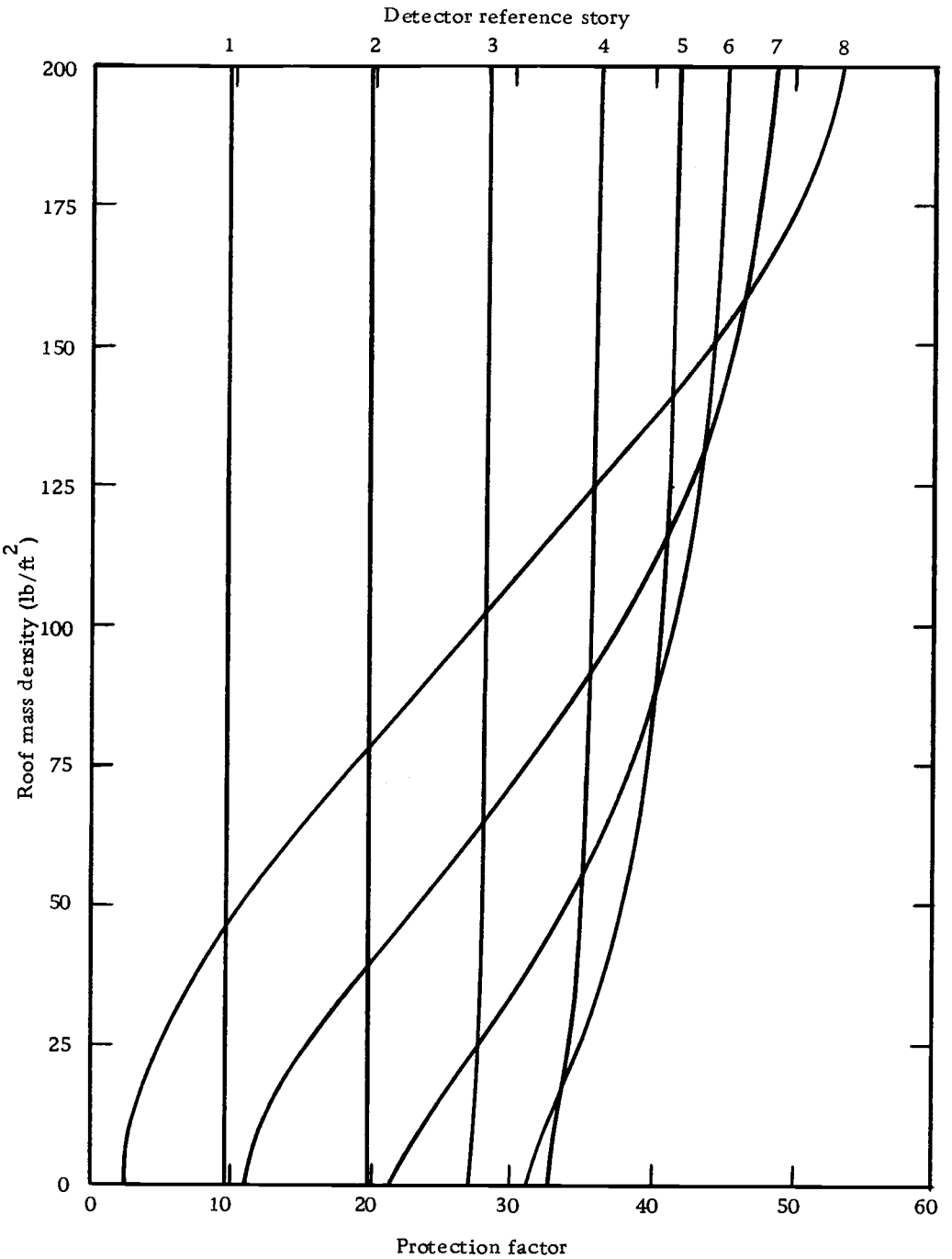

Figure 10. Variation of protection factor at each floor with roof density.

seventh story only experienced a 216% increase over the same range. Other floors experienced less change as they had the added benefit of intervening floors with distance from the overhead source.

Lower stories were not significantly affected by overhead contribution since ground radiation dominates as the detector approaches the ground plane. Thus the lower stories, in particular the bottom three, were not affected by changing the roof thickness. The fourth floor was little changed (7%) between 25 and 200 psf, while floor five increased by 32%.

From this it can be seen that little or no additional protection is gained in the major portion of the structure by increasing the roof thickness. Only the top few floors are affected. This would be even more evident if more stories were considered in the example. On the otherhand, however, the protection factor of a single story structure is greatly affected by roof mass as that is the only attenuating barrier between overhead source and detector.

Equivalent static seismic loads were computed by the U. B. C. equations. These are based on typical rigidity of the structural system and on mass, including dead load, of the structure. Total overturning moment at the base of the structure is not quite linear with roof mass in Figure 11 while total horizontal base shear is directly proportional to X_r in Figure 12. Seismic forces applied to a structure are simplified by the U. B. C. to be proportional to dead load

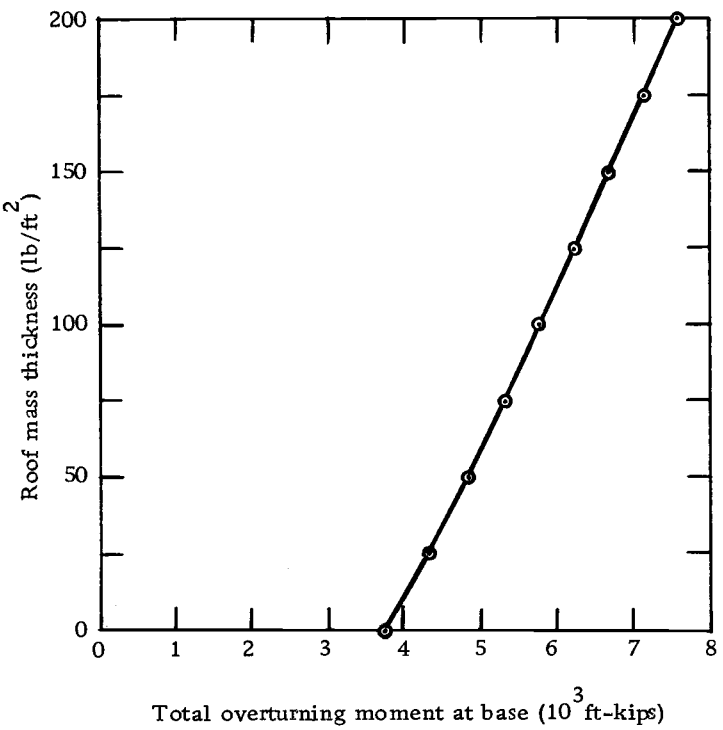

Figure 11. Total overturning moment at base due to seismic loading.

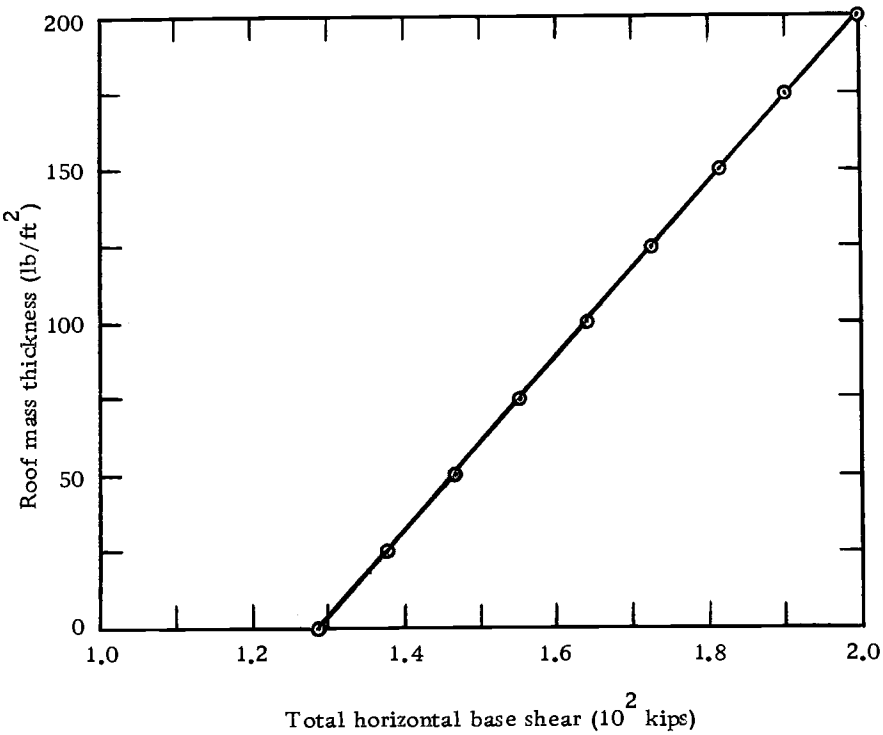

Figure 12. Total horizontal base shear due to seismic loading.

of the structure. So as the total building weight increases, applied shear and overturning moment must also increase.

Horizontal shearing forces to be applied at each floor level vary with both height and weight of the structure above a given point. Figure 13 shows how the horizontal force distributed at each floor varies with height above the base caused by changing the roof weight. This indicates that the force to be applied at the top of the structure is very sensitive to roof weight. Other floor shears are little affected by the roof weight but the effect does increase somewhat with height. The force at roof level increases by 544 % with an increase in roof mass thickness from 25 to 200 psf. Incidentally, there appears to be no particular structural phenomenon causing the plots to cross at a nearly common point. This is probably just a characteristic of the empirical distribution equation.

The overturning moment at each floor is caused by statically applying the horizontal shear forces at their own height above the level under consideration. Thus, as the floor loads increase, the overturning moments must increase. This will be more sensitive to increases in the upper floors because of static moment considerations. Curves are plotted in Figure 14 from data obtained from the U. B. C. equation for distribution of total overturning moment. Dashed lines extrapolating each curve to the base (zero height) level intersect a moment that matches the values of Figure 11 for total

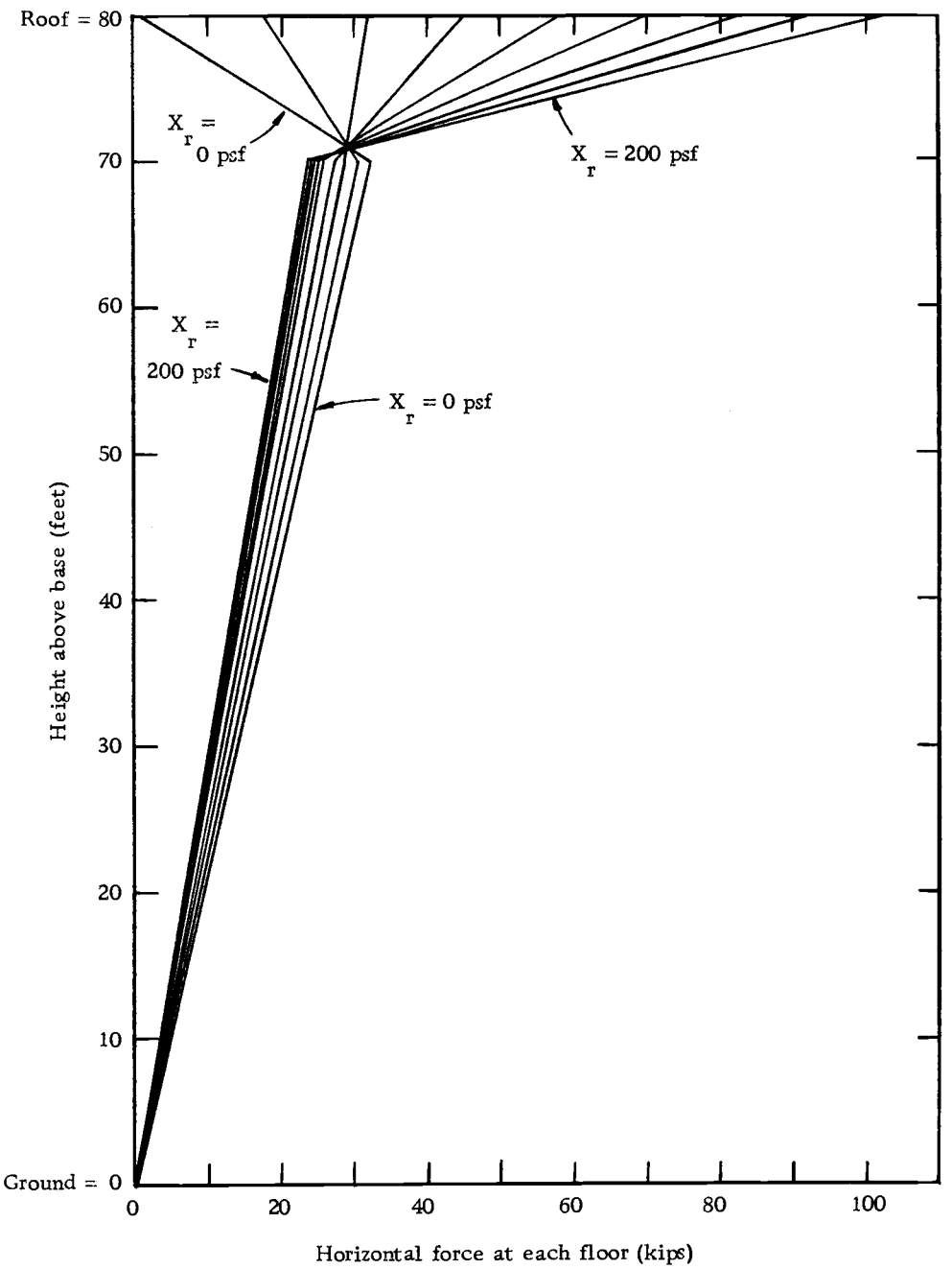

Figure 13. Horizontal force at each floor level due to seismic loading.

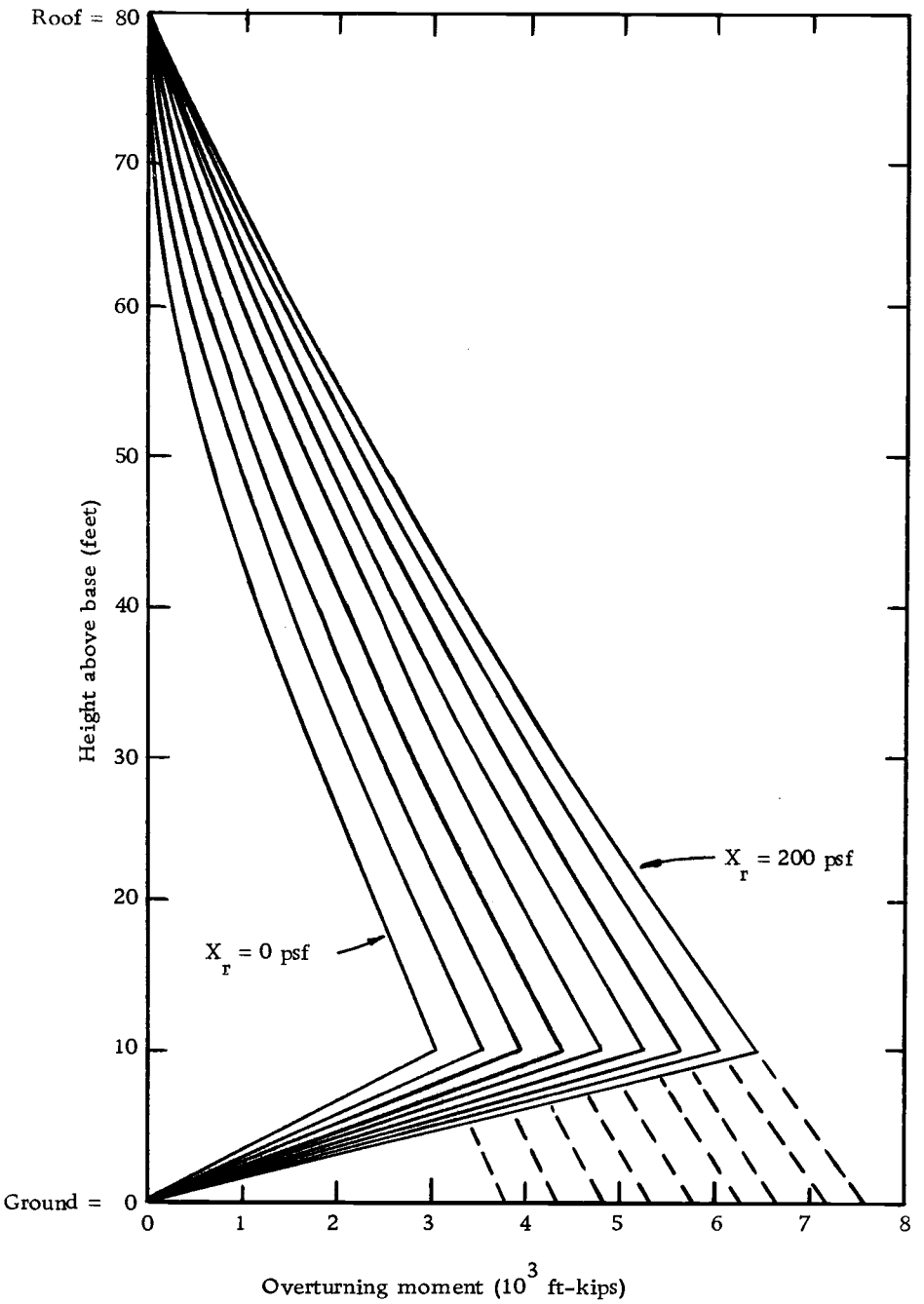

Figure 14. Overturning moment at each floor level.

overturning moments about the base for each value of roof weight.

Bending moments for each member and lateral building translation at each floor level were computed for the applied equivalent seismic forces. Maximumvalues of member moments and building deflection were presented in Table 2 as a function of roof mass thickness. Maximum building deflection is shown in Figure 15 as increasing at a positive, nonlinear rate with roof weight. This is to be expected because of the location of increasing dead load. If the total increase in building weight was uniformly distributed over the height, these deflection curves would approach straight lines. Deflection values are based on the relative member moments of inertia as shown previously in Figure 9. The middle curve of Figure 15 corresponds to a base stiffness of 60. The other two curves, shown for comparison purposes, are for base stiffnesses of 50 and 70. Recall that total member stiffness is obtained as the product of relative and base stiffness values.

As expected, total seismic deflection varies with both structural stiffness and weight of the structure. Based on a recommended maximum deflection of 12 inches per 1000 feet of height, the maximum allowable displacement for this example building is 0. 96 inches. Therefore, the total displacements computed are excessive, but are only for example purposes and could be easily varied by altering building stiffnesses.

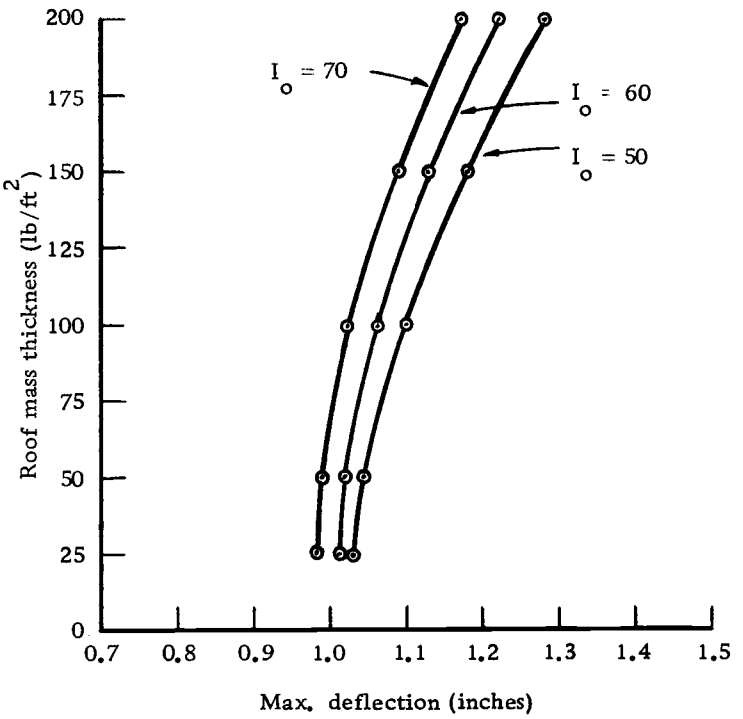

Figure 15. Maximum deflection of building.

The maximum moment occurring in any structural member for a base stiffness of 60 is shown in Figure 16. Maximum moments increase rapidly with roof mass thickness. An increase of 14.7% was experienced in a variation of roof weight from 25 to 200 psf. This is similar to the relationship for total overturning moment about the base as shown in Figure 11. In all cases of X_r, the maximum moments obtained were at the base of the three interior columns of the frame analyzed, and all were equal. All moments were checked against section properties of each member and were found to be

within the allowable limit.

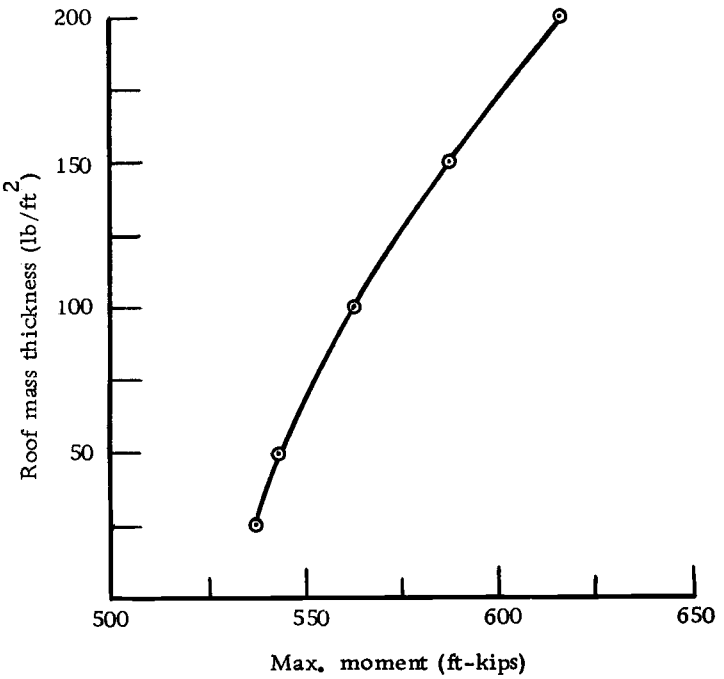

Figure 16. Maximum member moments.

The fundamental, or first, natural period of the structure was also determined by the program as a function of roof dead load. As shown in Figure 17, the period increases with weight of the structure. When a building becomes heavier for a given stiffness it will require a longer time to return to the initial position from a displaced position. The natural period, however, increases at a decreasing rate with roof weight. This shows the importance of another factor besides mass; namely, structural stiffness. Stiffness of the example building remained constant in this analysis, however, so all parameters were determined as a function of one variable only, the roof

weight.

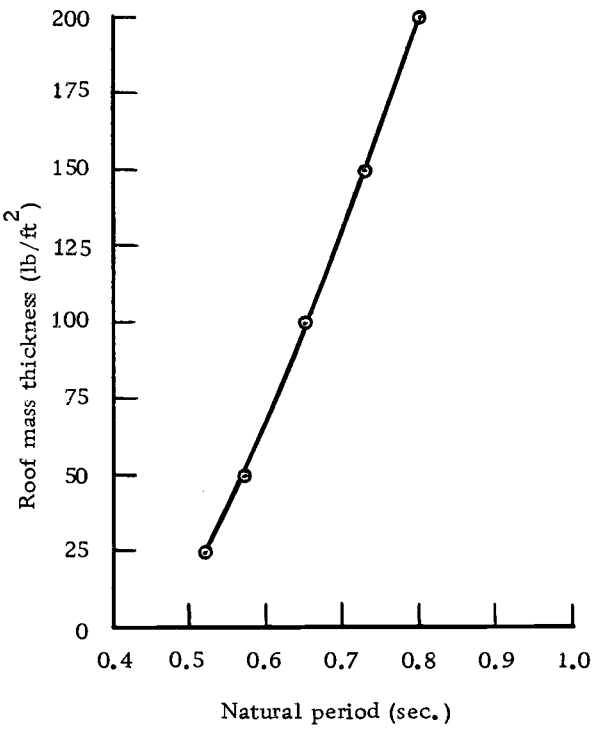

Figure 17. Fundamental period of building.

CONCLUSIONS AND RECOMMENDATIONS

In all cases, increasing the roof mass thickness resulted in increases of seismic structural analysis parameters. As dead weight of the structure increases so do applied horizontal seismic forces. This results in an increase in deflection of the structure and shears and moments within the structure.

Increasing the roof mass thickness, however, has little or no effect on radiation shielding potential for most floors of the structure. This contrast was more prominent with distance below the roof. Upper detector stories, and in particular the top two stories, were very much affected by added roof mass. Central and lower floors, however, experienced either a very low increase in protection factor or no increase at all.

The more stories a multistory structure contains, the more prominent will be the contrast in variation of parameters between seismic structural analysis and radiation protection factor analysis. Stresses and deflection from seismic disturbances are very sensitive to height and particularly to increases in mass at some significant height. But the protection factor of perhaps only the top five floors in a taller structure, say 20 stories, would be significantly influenced by even large increases in roof thickness. This low PF influence is due to overhead sources, which provide the major contribution in

upper stories, being reduced by the mass of each subsequent intervening floor level. Ground direct, of course, the major contributor in lower stories, is not affected by roof mass at any detector story. At the same time seismic stresses in this taller structure would be increased at a rapid rate with increases in roof weight.

Increases in stress and deflection of the structure with larger roof mass will require some increase in member stiffness. Also, some additional column size would be required to carry the heavier roof load. Yet all of this costly increase in size of structural members and time consuming extra design effort provides only small gains in fallout protection for only a small area of the building.

Therefore, for multistory structures it is impractical to provide fallout protection by merely increasing the roof thickness. Any protection factor increase must come from other sources, such as a more dense exterior covering than a thin curtainwall.

A minimum protection factor of 40 is recommended by O. C. D. for public structures. The example building did not provide this minimum for a reasonable roof weight anywhere except at the fifth or central floor with a roof mass density of 75 psf. This corresponds to a concrete slab thickness of 6 inches (probably impractical for the roof slab alone) or the conglomerate total of construction materials comprising the roof and ceiling which total 75 psf.

This study and building example show that the maximum

protection factor for a multistory structure occurs in the core region of the central stories for reasonable values of roof mass. With no additional attempts to increase the protection factor, this is the building area that should be equipped with fallout shelter facilities. Little or no change in design concepts or esthetics, however, need occur to provide minimum fallout protection in a multistory structure. For example, the use of a more dense curtainwall or other exterior wall barrier, or a better protected core region could greatly increase the protection factor. Awareness of the designer to "slant" the design toward providing fallout protection could increase the protection factor above minimum without any additional cost to the structure.

BIBLIOGRAPHY

1. Anderson, Paul. Statically indeterminate structures. New York, Ronald, 1953. 340 p.

2. Anderson, Paul and G. M. Nordby. Introduction to structural mechanics. New York, Ronald, 1960. 340 p.

3. Benjamin, J. R. Statically indeterminate structures. New York, McGraw-Hill, 1959. 350 p.

4. Biggs, J. M. Introduction to structural dynamics. New York, McGraw-Hill, 1964. 341 p.

5. Borg, S. F. and J. J. Gennaro. Advanced structural analysis. New Jersey, Van Nostrand, 1959. 368 p.

6. Glasstone, Samuel (ed.). The effects of nuclear weapons. Rev. ed. Washington, D. C., U. S. Atomic Energy Commission, 1964. 730 p.

7. Hall, A. S. and R. W. Woodhead. Frame analysis. New York, John Wiley, 1961. 247 p.

8. International Conference of Building Officials. Uniform building code. Vol. I. Pasadena, Cal., 1967. 595 p.

9. National Petroleum Council. Committee on Emergency Preparedness for the Petroleum Industry. Civil defense and emergency planning for the petroleum and gas industries. [Washington, D. C.] 1964. 59 p.

10. Price, B. T., C. C. Horton and K. T. Spinney. Radiation shielding. New York, Pergamen, 1957. 350 p.

11. Rogers, G. L. Dynamics of framed structures. New York, John Wiley, 1959. 355 p.

12. U. S. Atomic Energy Commission. Damage from atomic explosion and design of protective structures. Washington, D. C., 1950. 32 p.

13. U. S. Atomic Energy Commission. Radiation safety and major activities in the atomic energy programs, July-December 1956. [Washington, D. C.] 1957. 396 p.

14. U. S. Department of Defense. Office of Civil Defense. Shelter design and analysis. Vol. I. Fallout radiation shielding. Washington, D. C., 1967.

15. U. S. Department of the Interior. Defense Electric Power Administration. Civil defense preparedness in the electric power industry. Washington, D. C., 1966. 88 p.

16. U. S. Department of the Interior. Office of Minerals and Solid Fuels. Civil defense in the minerals and solid fuels industries. Washington, D. C., 1964. 32 p.

17. U. S. Federal Aviation Agency. Radiation safety for civil airports. [Washington, D. C.] 1957. 31 p. (AC 150/5240-6A)

18. U. S. Navy Department. Naval Radiological Defense Laboratory. Bureau of Ships. Principles of radiation and contamination control. Vol. 1. Washington, D. C., 1964. 70 p. (Navships 250-341-3)

19. White House Conference on Fallout Protection. Special Commission on Civil Defense of the Governors Conference. Washington, D. C., 1960. 37 p.

APPENDICES

Table A-1. Ground contribution to detector story 1.

	W	L	Z	e	n	ω	G_d	G_s	G_a
ω_o	40	80	77	0.500	1.925	0.074	---	---	---
ω_o'	120	160	77	0.750	0.967	0.300	---	---	---
ω_u''	120	160	27	0.750	0.338	0.664	---	0.310	0.074
ω_u'	120	160	17	0.750	0.213	0.780	---	0.235	0.059
ω_u	120	160	7	0.750	0.088	0.908	---	0.107	0.029
ω_ℓ	120	160	3	0.750	0.038	0.960	0.200	0.048	---

Detector story:	$G_g = 0.22670$		
	$C_g =$	0.099023	
First story above:	$G_g = 0.05764$		
	$C_g =$	0.002478	
Second story above:	$G_g = 0.04343$		
	$C_g =$	0.000360	$\Sigma C_g = 0.101861$

Table A-2. Ground contribution to detector story 2.

	W	L	Z	e	n	ω	G_d	G_s	G_a
ω_o	40	80	67	0.500	1.675	0.094	---	---	---
ω_o'	120	160	67	0.750	0.837	0.350	---	---	---
ω_u''	120	160	27	0.750	0.338	0.664	---	0.310	0.074
ω_u'	120	160	17	0.750	0.213	0.780	---	0.235	0.059
ω_u	120	160	7	0.750	0.088	0.908	---	0.107	0.029
ω_ℓ	120	160	3	0.750	0.038	0.960	0.069	0.048	---
ω_ℓ'	120	160	13	0.750	0.162	0.830	0.360	0.187	---

Detector story:	G_g = 0.11928		
	C_g =	0.038743	
First story above:	G_g = 0.05674		
	C_g =	0.001843	
Second story above:	G_g = 0.04343		
	C_g =	0.000268	
First story below:	G_g = 0.27352		
	C_g =	0.009328	ΣC_g = 0.050182

Table A-3. Ground contribution to detector story 3.

	W	L	Z	e	n	ω	G_d	G_s	G_a
ω_o	40	80	57	0.500	1.425	0.122	---	---	---
ω_o'	120	160	57	0.750	0.713	0.400	---	---	---
ω_u''	120	160	27	0.750	0.338	0.664	---	0.310	0.074
ω_u'	120	160	17	0.750	0.213	0.780	---	0.235	0.059
ω_u	120	160	7	0.750	0.088	0.908	---	0.107	0.029
ω_ℓ	120	160	3	0.750	0.038	0.960	0.034	0.048	---
ω_ℓ'	120	160	13	0.750	0.162	0.830	0.280	0.187	---
ω_ℓ''	120	160	23	0.750	0.288	0.709	0.450	0.285	---

Detector story:	G_g = 0.09058		
	C_g =	0.025363	
First story above:	G_g = 0.05674		
	C_g =	0.001589	
Second story above:	G_g = 0.04343		
	C_g =	0.000231	
First story below:	G_g = 0.23662		
	C_g =	0.006957	
Second story below:	G_g = 0.15171		
	C_g =	0.001402	ΣC_g = 0.035542

Table A-4. Ground contribution to detector story 4.

	W	L	Z	e	n	ω	G_d	G_s	G_a
ω_o	40	80	47	0.500	1.175	0.163	---	---	---
ω_o'	120	160	47	0.750	0.587	0.480	---	---	---
ω_u''	120	160	27	0.750	0.338	0.664	---	0.310	0.074
ω_u'	120	160	17	0.750	0.213	0.780	---	0.235	0.059
ω_u	120	160	7	0.750	0.088	0.908	---	0.107	0.029
ω_ℓ	120	160	3	0.750	0.388	0.960	0.020	0.048	---
ω_ℓ'	120	160	13	0.750	0.162	0.830	0.230	0.187	---
ω_ℓ''	120	160	23	0.750	0.288	0.709	0.400	0.285	---

Detector story:	$G_g = 0.07910$		
	$C_g =$	0.019491	
First story above:	$G_g = 0.05674$		
	$C_g =$	0.001398	
Second story above:	$G_g = 0.04343$		
	$C_g =$	0.000203	
First story above:	$G_g = 0.20710$		
	$C_g =$	0.005358	
Second story above:	$G_g = 0.16401$		
	$C_g =$	0.001334	$\Sigma C_g = 0.027784$

Table A-5. Ground contribution to detector story 5.

	W	L	Z	e	n	ω	G_d	G_s	G_a
ω_o	40	80	37	0.500	0.925	0.227	---	---	---
ω_o'	120	160	37	0.750	0.462	0.560	---	---	---
ω_u''	120	160	27	0.750	0.338	0.664	---	0.310	0.074
ω_u'	120	160	17	0.750	0.213	0.780	---	0.235	0.059
ω_u	120	160	7	0.750	0.088	0.908	---	0.107	0.029
ω_ℓ	120	160	3	0.750	0.038	0.960	0.016	0.048	---
ω_ℓ'	120	160	13	0.750	0.162	0.830	0.185	0.187	---
ω_ℓ''	120	160	23	0.750	0.288	0.709	0.360	0.285	---

Detector story:	G_g = 0.07582		
	C_g =	0.016984	
First story above:	G_g = 0.05674		
	C_g =	0.001271	
Second story above:	G_g = 0.04343		
	C_g =	0.000185	
First story below:	G_g = 0.17348		
	C_g =	0.004080	
Second story below:	G_g = 0.16811		
	C_g =	0.001243	ΣC_g = 0.023763

Table A-6. Ground contribution to detector story 6.

	W	L	Z	e	n	ω	G_d	G_s	G_a
ω_o	40	80	27	0.500	0.675	0.328	---	---	---
ω_o'	120	160	27	0.750	0.338	0.664	---	0.310	0.074
ω_u'	120	160	17	0.750	0.213	0.780	---	0.235	0.059
ω_u	120	160	7	0.750	0.088	0.908	---	0.107	0.029
ω_ℓ	120	160	3	0.750	0.038	0.960	0.014	0.048	---
ω_ℓ'	120	160	13	0.750	0.162	0.830	0.170	0.187	---
ω_ℓ''	120	160	23	0.750	0.288	0.709	0.325	0.285	---

Detector story:	G_g = 0.07418		
	C_g =	0.015370	
First story above:	G_g = 0.05674		
	C_g =	0.001176	
Second story above:	G_g = 0.04343		
	C_g =	0.000171	
First story below:	G_g = 0.16282		
	C_g =	0.003542	
Second story below:	G_g = 0.14351		
	C_g =	0.000981	ΣC_g = 0.021240

Table A-7. Ground contribution to detector story 7.

	W	L	Z	e	n	ω	G_d	G_s	G_a
ω_o	40	80	17	0.500	0.425	0.495	---	---	---
ω_o'	120	160	17	0.750	0.213	0.780	---	0.235	0.059
ω_u	120	160	7	0.750	0.088	0.908	---	0.107	0.029
ω_ℓ	120	160	3	0.750	0.038	0.960	0.013	0.048	---
ω_ℓ'	120	160	13	0.750	0.162	0.830	0.150	0.187	---
ω_ℓ''	120	160	23	0.750	0.288	0.709	0.300	0.285	---

Detector story:	G_g = 0.07336		
	C_g =	0.014718	
First story above:	G_g = 0.05674		
	C_g =	0.001112	
First story below:	G_g = 0.14724		
	C_g =	0.003030	
Second story below:	G_g = 0.14761		
	C_g =	0.000960	ΣC_g = 0.019820

Table A-8. Ground contribution to detector story 8.

	W	L	Z	e	n	ω	G_d	G_s	G_a
ω_o	40	80	7	0.500	0.175	0.760	---	---	---
ω_o'	120	160	7	0.750	0.088	0.908	---	0.107	0.029
ω_ℓ	120	160	3	0.750	0.038	0.960	0.012	0.048	---
ω_ℓ'	120	160	13	0.750	0.162	0.830	0.135	0.187	---
ω_ℓ''	120	160	23	0.750	0.288	0.709	0.280	0.285	---

Detector story:	G_g = 0.07254		
	C_g =	0.013405	
First story below:	G_g = 0.13576		
	C_g =	0.002635	
Second story below:	G_g = 0.14351		
	C_g =	0.000875	ΣC_g = 0.016915

Table A-9. Overhead contribution and protection factors.

$$C_o = C_o(\omega_o, X_{oT}) + [C_o(\omega_o', X_{oT}) - C_o(\omega_o, X_{oT})]B_i'(X_i) \qquad RF = C_o + C_g$$

Floor	ω_o	ω_o'	X_{oT}	$C_o(\omega_o', X_{oT})$	$C_o(\omega_o, X_{oT})$	C_o	RF	PF
8	0.760	0.908	0	0.500	0.250	0.3562	0.3731	2.7
			25	0.170	0.145	0.1982	0.2151	4.7
			40	0.095	0.090	0.0921	0.1090	9.2
			50	0.080	0.075	0.0771	0.0940	10.6
			75	0.038	0.037	0.0374	0.0543	18.4
			100	0.020	0.020	0.0200	0.0369	27.1
			125	0.011	0.011	0.0110	0.0279	35.8
			150	0.0058	0.0057	0.0057	0.0226	44.3
			175	0.0032	0.0030	0.0030	0.0199	50.2
			200	0.0018	0.00175	0.0018	0.0187	53.5
7	0.495	0.780	40	0.085	0.063	0.0724	0.0892	11.2
			65	0.048	0.044	0.0457	0.0655	15.3
			80	0.032	0.028	0.0297	0.0495	20.2
			90	0.025	0.022	0.0233	0.0431	23.2
			115	0.014	0.012	0.0129	0.0327	30.6
			140	0.0073	0.0067	0.0070	0.0268	37.4
			165	0.0039	0.0036	0.0037	0.0235	42.0
			190	0.0022	0.0020	0.0021	0.0219	45.7
			215	0.0013	0.0012	0.0013	0.0211	47.4
			240	0.0007	0.00068	0.0007	0.0205	48.8

(Continued)

Table A-9. (Continued)

Floor	ω_o	ω_o'	X_{oT}	$C_o(\omega_o', X_{oT})$	$C_o(\omega_o, X_{oT})$	C_o	RF	PF
6	0.33	0.664	80	0.031	0.021	0.0253	0.0471	21.2
			105	0.017	0.012	0.0141	0.0359	27.8
			120	0.012	0.0083	0.0099	0.0317	31.6
			130	0.0090	0.0066	0.0077	0.0295	33.9
			155	0.0048	0.0039	0.0043	0.0261	38.3
			180	0.0026	0.0022	0.0024	0.0242	41.3
			205	0.0016	0.0013	0.0014	0.0232	43.1
			230	0.00090	0.00078	0.0008	0.0226	44.2
			255	0.00050	0.00045	0.0005	0.0223	44.9
			280	0.00029	0.00026	0.0003	0.0221	45.3
5	0.227	0.56	120	0.0115	0.0064	0.0084	0.0322	31.0
			145	0.0060	0.0040	0.0049	0.0287	34.8
			160	0.0040	0.0028	0.0033	0.0271	35.6
			170	0.0033	0.0022	0.0027	0.0265	37.8
			195	0.0019	0.0014	0.0016	0.0254	39.4
			220	0.00115	0.00080	0.0008	0.0246	40.6
			245	0.00062	0.00048	0.0005	0.0243	41.1
			270	0.00035	0.00028	0.0003	0.0241	41.5
			295	0.00020	0.00017	0.0002	0.0240	41.7
			320	0.00011	0.00011	0.0001	0.0239	41.8

(Continued)

Table A-9. (Continued)

Floor	ω_o	ω_o'	X_{oT}	$C_o(\omega_o', X_{oT})$	$C_o(\omega_o, X_{oT})$	C_o	RF	PF
4	0.163	0.480	160	0.0039	0.0022	0.0029	0.0307	32.6
			185	0.0022	0.0016	0.0019	0.0297	33.7
			200	0.0016	0.00095	0.0012	0.0290	34.5
			210	0.0013	0.00076	0.0010	0.0288	34.7
			235	0.00075	0.00048	0.0006	0.0284	35.2
			260	0.00043	0.00028	0.0003	0.0281	35.6
			285	0.00030	0.00017	0.0002	0.0280	35.7
			310	0.00015	0.000115	0.0001	0.0279	35.8
			335	---	---	---	0.0278	36.0
			360	---	---	---	0.0278	36.0
3	0.122	0.400	200	0.0016	0.00079	0.0012	0.0367	27.2
			225	0.00090	0.00047	0.0007	0.0362	27.6
			240	0.00066	0.00035	0.0005	0.0360	27.8
			250	0.00052	0.00028	0.0004	0.0359	27.9
			275	0.00030	0.00017	0.0002	0.0357	28.0
			300	0.00017	0.00011	0.0001	0.0356	28 1
			325	---	---	---	0.0355	28.2
			350	---	---	---	0.0355	28.2
			375	---	---	---	0.0355	28.2
			400	---	---	---	0.0355	28.2

(Continued)

Table A-9. (Continued)

Floor	ω_o	ω_o'	X_{oT}	$C_o(\omega_o', X_{oT})$	$C_o(\omega_o, X_{oT})$	C_o	RF	PF
2	0.094	0.35	240	0.00062	0.00029	0.0004	0.0506	19.9
			265	0.00036	0.00017	0.0003	0.0505	19.9
			280	0.00026	0.00013	0.00025	0.0504	19.9
			290	0.00021	0.00011	0.0002	0.0504	19.9
			315	0.00013	0.00007	0.0001	0.0503	19.9
			340	---	---	---	0.0502	19.9
1	0.074	0.30	280	0.00025	0.00011	0.0002	0.1021	9.8
			305	0.00015	0.00006	0.0001	0.1020	9.8
			320	---	---	---	0.1019	9.8
			330	---	---	---	0.1019	9.8